Fermilab Library
0 1160 0019626 5

CPT-92-P-2816

Physique Théorique Marseille

DO WE UNDERSTAND POLARIZATION PHENOMENA IN HIGH ENERGY PHYSICS ?*

Jacques Soffer

Unité Propre de Recherche 7061

November 1992
CPT-92/P.2816

FERMILAB
DEC 11 1992
LIBRARY

* Lectures given at the RCNP-Kikuchi School on Spin Physics at Intermediate Energies, Osaka, Japan, November 16-19, 1992

CNRS Luminy – Case 907 – CPT – F 13288 Marseille Cedex 9 – France

1. INTRODUCTION

The importance of spin in high energy hadron physics has not yet been fully appreciated in spite of numerous striking experimental facts recently observed in many different reactions. This reflects the widespread prejudice that spin is an inessential complication. It is based on the fact that according to naive arguments, when the available energy increases in hadronic collisions, the masses of the particles involved become negligible, so one should expect all fermions to behave like massless neutrinos with trivial helicity properties. As a result in particular no ***transverse spin effects*** should survive at high energy and we will see that experimental data do not support at all this over simplified picture because, first some of these spin effects are and remain non zero as the energy increases and second, there are some which are even growing with energy. We will see that spin effects are puzzling and must play a genuine role in our understanding of strong interactions dynamics. We believe that they should motivate new theoretical efforts because they contain a unique information which can help to clarify some key physics issues. Although, part of this information is burried in unpolarized cross sections, one must remember that for consistency, these basic observables in the first place, should be well described by any sensible theoretical approach of spin effects. In what follows, we will strongly emphasize this point and we will also stress the relevance of interference mechanisms for the description of some transverse spin effects both in exclusive and inclusive hadronic reactions.

Polarized deep inelastic scattering allows to learn about, how the proton spin is shared among its constituents, more precisely about their helicity distributions, and the existing data has led to various theoretical interpretations from which have emerged different pictures of the proton spin structure. We will also mention the relevance of Drell-Yan lepton pair production with polarized beams for learning about quark and antiquarks transversity distributions.

The outline of these lectures is as follows. In the next section we will consider spin effects in exclusive reactions, successively at small and large scattering angles, this last kinematical region allowing to probe hadronic properties at very short distances. In section 3 we turn to spin dependence in inclusive reactions and we will first mention the problem of the single helicity asymmetry related to parity violation as a test of the electroweak standard model. We then discuss several single transverse spin asymmetries in particular in hyperon production in the fragmentation region corresponding to small transverse momentum ($p_T \leq 1$ GeV/c). We will also consider the central region and large p_T and some double helicity asymmetries. In section 4 we will discuss polarized structure functions both in leptoproduction and in Drell-Yan lepton pair production and the important issues related to the proton spin problem. Concluding remarks are given in the last section.

2. SPIN IN EXCLUSIVE REACTIONS

2.1. *The small scattering angle region*

This is the region which is dominated by soft physics and many different dynamical approaches give a reasonable account of medium energy phenomenology in this kinematical region [1]. Let us first recall, some simple ideas based on the so-called naïve (non-relativistic) quark model. Each hadronic scattering amplitude is represented by the coherent sum of all possible quark-quark scattering amplitudes assuming that only one quark in each particle can interact at a time and possibly flip its spin. The remaining (or spectator) quarks do not affect the scattering except that they afterwards recombine with the interacting quarks to form the final hadrons. As a consequence it is possible to relate meson-baryon and baryon-baryon reactions since they both proceed through the same quark-quark amplitudes. In particular, one can relate the two inelastic reactions $pp \to \Delta^{++}n$ and $K^+n \to K^{*0}p$, both exotic in the direct channel and having the same Regge exchanges in the t-channel. From the original sixteen amplitudes describing $pp \to \Delta^{++}n$, ten of them vanish and one is left with the same number of amplitudes characterizing $K^+n \to K^{*0}p$. So one gets, for example, interesting relations between the density matrix elements of K^{*0} and of the Δ^{++} which are in fair agreement with the 6 GeV/c data as shown in Fig.1[1].

[1] For a more complete analysis in different helicity frames, see ref.[3].

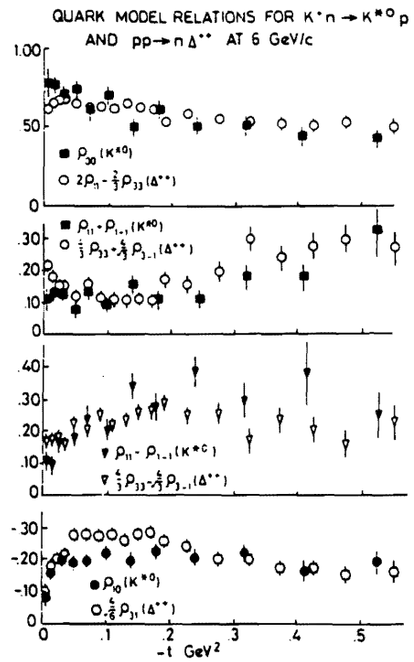

Fig.1 Quark model predictions of the relations between the density matrix elements of $K^+n \to K^{*0}p$ and $pp \to \Delta^{++}n$ at 6 GeV/c (data from ref.[2]).

Let us now consider nucleon-nucleon scattering. We recall that nucleon-nucleon elastic scattering is described in terms of five independent helicity amplitudes $\phi_i (i \doteq 1, \ldots 5)$ usually denoted as follows: $\phi_1 =< ++|++ >$, $\phi_2 =< ++|-- >$, $\phi_3 =< +-|+- >$, $\phi_4 =< +-|-+ >$ and $\phi_1 =< ++|+- >$. We will be concerned with the following set of observables defined in ref.[1] whose expressions in terms of the ϕ_i's are

$$
\begin{aligned}
\sigma_0 &= s^2 d\sigma/dt = 1/2[|\phi_1|^2 + |\phi_2|^2 + |\phi_3|^2 + |\phi_4|^2 + 4|\phi_5|^2] \\
A &= Im[(\phi_1 + \phi_2 + \phi_3 - \phi_4)\phi_5^*]/\sigma_0 \\
A_{NN} &= Re(\phi_1\phi_2^* - \phi_3\phi_4^* + 2|\phi_5|^2)/\sigma_0 \\
D_{NN} &= Re(\phi_1\phi_3^* - \phi_2\phi_4^* + 2|\phi_5|^2)/\sigma_0 \\
K_{NN} &= Re(\phi_3\phi_2^* - \phi_1\phi_4^* + 2|\phi_5|^2)/\sigma_0 \\
A_{LL} &= -[|\phi_1|^2 + |\phi_2|^2 - |\phi_3|^2 - |\phi_4|^2]/2\sigma_0 \\
A_{SS} &= Re(\phi_1\phi_2^* + \phi_3\phi_4^*)/\sigma_0 \\
A_{LS} &= Re[(\phi_1 + \phi_2 - \phi_3 + \phi_4)\phi_5^*]/\sigma_0 \quad .
\end{aligned}
\tag{1}
$$

$d\sigma/dt$ is the unpolarized cross section, A is called the ***analyzing power*** (or single transverse spin asymmetry) and A_{NN} the ***transverse spin-spin correlation parameter***. In the small angle region the relevant framework is the classic Regge theory which provides a simple description of the analyzing power A in a two-body elastic reaction in terms of an ***interference mechanism*** between the non-flip amplitude, mainly imaginary, dominated by the Pomeron exchange and a flip amplitude whose phase is related to that of the dominant Regge exchange. As a consequence, at a fixed t-value, A decreases with increasing energy following the general trend of the data. In pp elastic scattering at high energies A is non-zero as shown in Fig.2 and one may wonder about the Pomeron helicity-flip. The unpolarized cross section $d\sigma/dt$ is well described by the impact picture approach [5] in a very broad energy range. In Fig.3 we recall a confrontation of the model (solid curve) with the best available data at 24 GeV/c showing that indeed diffractive scattering dominates up to $|t| \simeq 4$ GeV^2, but then it clearly goes below the data. The spin dependence was introduced in the model by assuming the existence of a hadronic matter current inside a polarized proton. Hadronic motion along the direction of the incident beam hitting the polarized proton is described by a velocity distribution $\omega(b)$ which is a function of the impact parameter b. In the absence of any precise determination of this function, one chooses arbitrarily a Gaussian form $\omega(b) = \omega_0 \exp\left(-b^2/b_0^2\right)$ which leads to the predictions

shown in Fig.2. Although the errors in the data are large, there is an indication for a larger polarization at higher t-values.

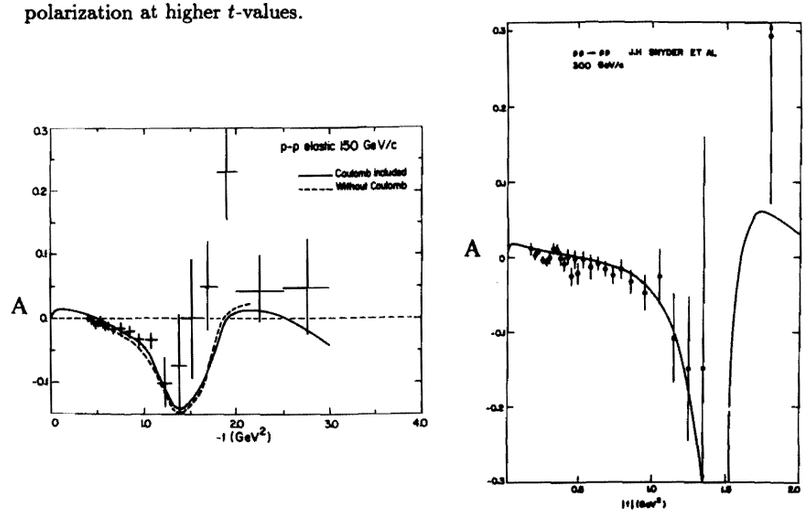

Fig.2 pp elastic analyzing power at p_{lab} = 150 and 300 GeV/c. Data from ref.[4] and model predictions from ref.[5].

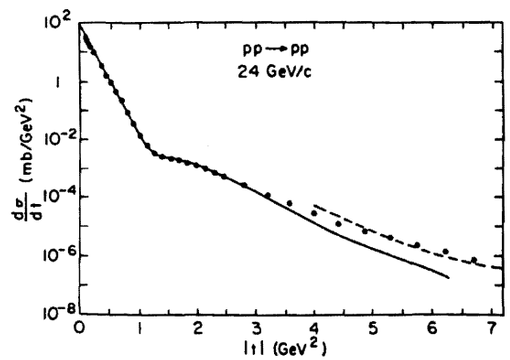

Fig.3 pp elastic scattering data from ref.[6]. Solid and dashed curves are explained in the text.

2.2. *The large scattering angle region*

In the large angle region there is a fair amount of data in nucleon-nucleon elastic scattering. First let us recall that one can express in terms of A and A_{NN} the ratio of spin-parallel to spin-antiparallel cross sections as follows

$$\frac{\sigma\uparrow\uparrow}{\sigma\uparrow\downarrow} = \frac{1+2A+A_{NN}}{1-A_{NN}} \tag{2}$$

and one sees on an interesting plot (see Fig.4) how this ratio varies against p_T^2 and p_{lab}

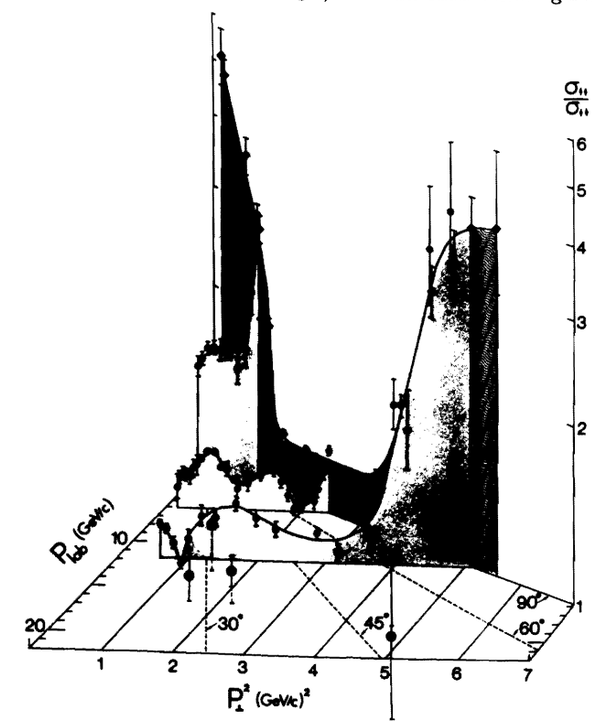

Fig.4 Three dimensional plot for $\sigma_{\uparrow\uparrow}/\sigma_{\uparrow\downarrow}$ against p_T^2 and p_{lab} showing also the fixed $\theta_{c.m.}$ behaviour from ref.[7].

showing clearly that spin effects do not vanish at high energy and large p_T^2. Let us recall some remarkable features of data, first at fixed energy. At $p_{lab} = 24$ GeV/c (see Fig.3), after the characteristic narrow diffraction peak, $d\sigma/dt$ has a slower fall off in t up to $\theta_{c.m.} = 45^o$. At 6 GeV/c the analyzing power for np elastic scattering is negative at large angles and of the order of -40% near 90° (see Fig.5). For pp elastic scattering at 28 GeV/c, A is of the order of 5% or so in the small angle region but increases to a much higher positive value for $\theta_{c.m.} \sim 45^o$ as shown in Fig.6. At fixed angle $d\sigma/dt$ near 90° has a very fast drop off with energy up to 20 GeV/c or more (see Fig.7) and A_{NN} has a dramatic rise above 8 GeV/c up to 60% at the highest energy ever measured as shown in Fig.8. At $\theta_{c.m.} = 50^o$ (see Fig.9) the behavior of A suggests the appearance of a new regime for $p_{lab} > 20$ GeV/c which remains to be confirmed by the measurement of A_{NN} at higher energy. Is there a simple interpretation of all these experimental facts? As we said before, the scattering amplitudes constructed in the framework of the impact picture model provide an accurate representation of the soft-part of the scattering process which allows a fair description of $d\sigma/dt$ at the PS energy, up to $|t| \simeq 4$ GeV^2 as shown by the solid curve in Fig.3. Beyond this t-value the diffractive contribution drops faster than the data, suggesting that it cannot be the "whole story" since the hard-part of the scattering becomes important at large angles and should be included to complete the physical picture.

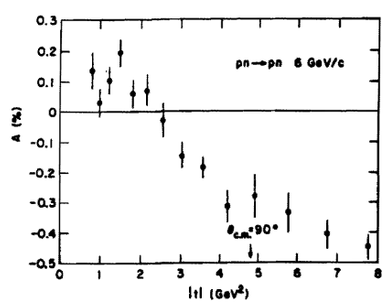

Fig.5 The analyzing power A for np elastic scattering at 6 GeV/c from ref.[8].

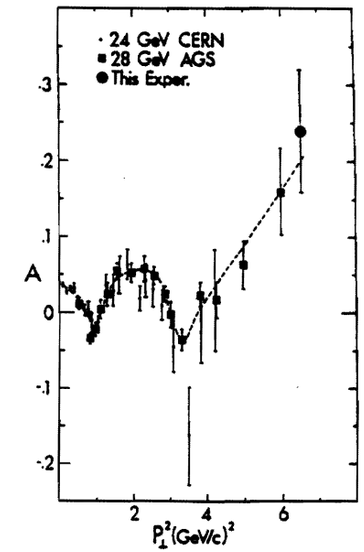

Fig.6 The analyzing power A for pp elastic scattering versus $p_\perp^2$ taken from ref.[9]. The curve is hand-drawn to guide the eye.

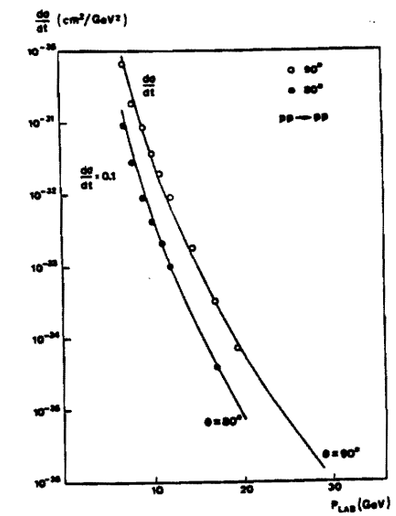

Fig.7 pp elastic scattering data at large angles from ref.[10]. The curves are explained in the text.

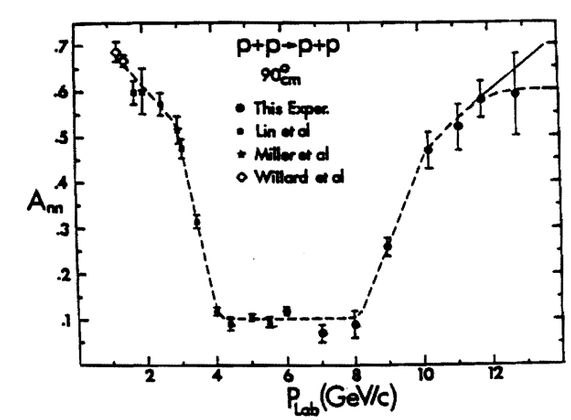

Fig.8 The A_{NN} parameter for pp elastic scattering at $\theta_{c.m.} = 90^o$ versus p_{lab} from ref.[11]. The curve is hand-drawn to guide the eye.

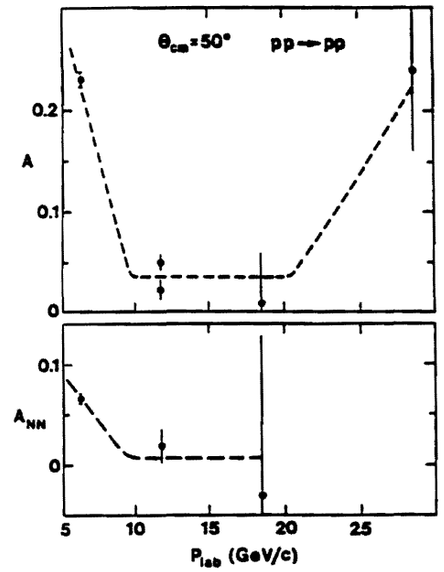

Fig.9 pp polarization parameters A and A_{NN} versus p_{lab} for $\theta_{c.m.} = 50°$ (data from refs.[12] and [13]). The curves are hand drawn to guide the eye.

Before we discuss different possibilities, let us make some remarks about the special case of pp elastic scattering at 90°. Like in the forward direction, life is simpler because only three amplitudes survive since $\phi_3 = -\phi_4$ and $\phi_5 = 0$. So instead of twenty five observables resulting from the initial five amplitudes, we have only nine observables; eight of them vanish (e.g. $A = 0$) and there are eight linear relations e.g.

$$D_{NN} = K_{NN} \quad \text{and} \quad 1 + A_{LL} = A_{NN} - A_{SS} \quad . \tag{3}$$

In addition there exist special positivity relations, generalizations of the obvious constraint $|A| \leq 1$, like for example

$$|D_{NN}| \leq \frac{1 + A_{NN}}{2} \quad . \tag{4}$$

Knowing A_{NN} and A_{LL}, eqs.(3) and (4) can be used to predict A_{SS} and to put limits on $|D_{NN}|$. These relations, which are a guide for experimentalists, should be satisfied by

any dynamical assumptions. Clearly they don't hold for np elastic scattering because of non-identical particles.

One possible theoretical framework is perturbative QCD predicting for the cross section of any exclusive process $a + b \to c + d$, the asymptotic scaling law

$$\frac{d\sigma}{dt} = s^{-n} F(\theta_{c.m.}) \tag{5}$$

with $n = 10$ for baryon-baryon scattering. This rapid energy dependence is in reasonable agreement with the data shown in Fig.9. However the exact expression of $F(\theta_{c.m.})$ providing both the absolute normalization and the angular dependence of $d\sigma/dt$ involves in perturbative QCD an impressive number of lowest order diagrams (see ref.[14]) and is not yet available. Note that according to the data of ref.[15] on $\gamma\gamma \to \pi^+\pi^-$, K^+K^- and $\bar{p}p$, the predicted normalization is wrong by a substantial factor. There is another problem when one compares baryon-baryon and baryon-antibaryon scattering as shown in Fig.10.

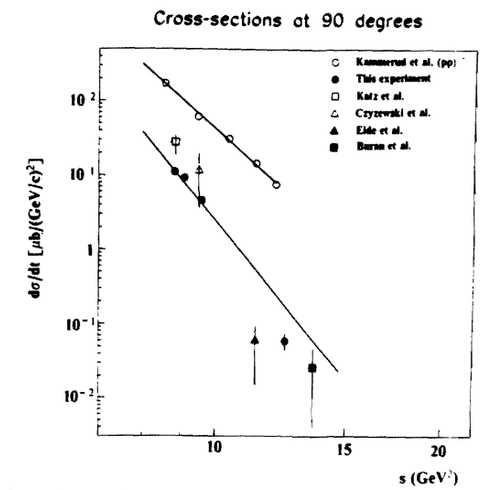

Fig.10 The pp and $p\bar{p}$ elastic differential cross-sections at $\theta_{c.m.} = 90°$ as a function of s (taken from ref.[16]).

The pp data fit to s^{-9} and this line extrapolates reasonably well to the data at $p_{lab} = 10$ GeV/c obtained at BNL [17] i.e. $(48 \pm 5)nb/(\text{GeV/c})^2$. However the $\bar{p}p$ data fall more rapidly than the lower curve which is s^{-12} and this is consistent with some upper limits obtained at higher energies.

There is another simple feature of perturbative QCD that one ought to test with the spin dependent observables that is the *helicity conservation rule* [18]. The sum of the initial helicities must be equal to the sum of the final ones

$$\lambda_a + \lambda_b = \lambda_c + \lambda_d \tag{6}$$

as a consequence of the vectorial nature of the gluon and of the chiral limit for light quarks. For both pp and np elastic scattering this rule implies that the amplitudes ϕ_2 and ϕ_5 must be zero at large angles. Let us examine several consequences of this restrictive situation at large angles in addition to the fact that the helicity amplitudes resulting from perturbative QCD are expected to be essentially real, although this last assumption can be relaxed as we will see later.

i) the analyzing power A must vanish because it is linear in ϕ_5 (see eq.(1)), but this is obviously not verified by the data presented earlier.

ii) there are new constraints between the double spin correlation parameters for example

$$A_{SS} = -A_{NN}$$

and

$$\left|\begin{matrix} D_{NN} \\ K_{NN} \end{matrix}\right| = \sqrt{\frac{1}{2}(1 - A_{LL})(1 + A_{LL} \pm \sqrt{(1 + A_{LL})^2 - 4A_{NN}^2})} \tag{7}$$

so by measuring A_{NN} and A_{LL} it is possible to predict A_{SS}, $|D_{NN}|$ (or $|K_{NN}|$) which are consistency checks. At 11.75 GeV/c, the data does not satisfy this, because in particular for $\theta_{c.m.} > 65°$ one has [19]

$$(1 + A_{LL} - 2A_{NN})/4 = (-0.072 \pm 0.02) \tag{8}$$

which, according to eq.(7), should be a positive quantity!

iii) A_{NN} has now a much simpler form and reads

$$A_{NN} = \frac{-2\phi_3\phi_4}{\phi_1^2 + \phi_3^2 + \phi_4^2} \quad . \tag{9}$$

At this stage one may ask the following question: is it easy to understand the rapid variation seen in the data namely $A_{NN} \sim 0$ at 50° and $A_{NN} \sim 60°$ at 90°? From eq.(9) one needs either $\phi_3/\phi_1 \sim 0$ or $\phi_4/\phi_1 \sim 0$ at 50° and $\phi_3/\phi_1 = -\phi_4/\phi_1 = \sqrt{3/2}$ at 90°. In most models $\phi_3/\phi_1 \sim 1$ ***at all angles***, so the ratio of the double flip amplitude ϕ_4 to the non flip amplitude ϕ_1 should vary quickly between 50° and 90°. Another consequence of $\phi_1 \sim \phi_3$, provided ϕ_5 is not zero, is the fact that A_{LS} defined in eq.(1) is expected to be very small for all angles in agreement with experimental observation [19].

The constituent-interchange model [20] which satisfies the helicity conservation rule is even more restrictive because one has

$$\begin{aligned} \phi_1 &= \phi_3 - \phi_4 \\ \phi_3 &= 56\ f(\theta_{c.m.}) + 68\ f(\pi - \theta_{c.m.}) \\ \phi_4 &= -68\ f(\theta_{c.m.}) - 56\ f(\pi - \theta_{c.m.}) \end{aligned} \tag{10}$$

with

$$f(\theta_{c.m.}) = 0.5/(1 - \cos\theta_{c.m.})^4 \quad .$$

It leads to A_{NN} (90°)=1/3 and almost the same value at 50°, in complete contradiction with the 12 GeV/c data [11].

We regard this situation as an evidence for serious need of non-perturbative effects in a kinematic region where pertubative QCD is believed to be relevant ! The difficulties mentioned above do not appear in the framework of Quark Geometro Dynamics (QGD) whose applications to large angle scattering has been discussed elsewhere [21]. This approach displays many features of the naive quark model. The two-body large-angle amplitudes are

obtained by folding the hadron vertex functions with the elementary quark-quark scattering amplitudes. The vertex functions are constructed with the assumption that during the scattering process the initial and final baryons have in common two spectator quarks which conserve spin, momentum and the internal degrees of freedom. The energy dependence of the vertex functions is consistent with the large Q^2 behavior of the hadron form factors. At the level of the basic quark-quark amplitudes it is assumed that the short-distance force (which is color neutral) is generated by the exchange of several infinite towers of mesons, which are not only transverse vector states (analogous to gluons in perturbative QCD), but also pseudoscalar and longitudinal vector states. As a consequence, the spin structure of the amplitudes is not as restrictive as that of perturbative QCD and does not obey the helicity conservation rule eq.(6). Therefore one obtains a set of five real amplitudes given in Table 1 of ref. [21] which allows a good description of $d\sigma/dt$ near 90° as shown by the solid curves in Fig.7. The model does not provide the absolute normalization which was fixed at 10 GeV/c and 90°. By simply adding these contributions to the impact picture amplitude one gets the dashed line shown in Fig.3 in better agreement with the data for $|t| > 5$ GeV^2 or so. For $p_{lab} = 28.7$ GeV/c at the highest available t-value, $|t| = 10$ GeV^2, we find $d\sigma/dt = 3.7 \times 10^{-8} mb/$ GeV^2 which can be compared with the data $d\sigma/dt = (3.5 \pm .7)10^{-8} mb/$ GeV^2 reported in ref.[10]. If we now calculate the analysing power A at 28 GeV/c we find a rapid increase near $\theta_{c.m.} = 45°$ up to 30° or so in agreement with the data as shown in Fig.11. This large effect is due to a maximum interference between the hard scattering amplitudes which are real and the dominantly imaginary impact picture contribution. The arrow indicates that below $p_T^2 = 5$ GeV^2, the solid line turns to a broken line which is not a reliable prediction. In Fig.11 we also show our prediction for A at 50 GeV/c which is reliable down to $p_T^2 = 2$ GeV^2 or so because the cross section is also well described down to smaller p_T^2 values as shown in Fig.12. The predictions for A_{NN} exhibit a rise to about 100% near 90° as displayed in Fig.13. Many other interesting predictions for pp and np elastic scattering can be found in ref.[22]. Let us emphasize that if these predictions for A and A_{NN} turn out to be verified, they would confirm the correctness of the phase of the impact picture and of the magnitude of the

hard scattering single flip amplitude ϕ_5. Higher-order twist effects have been invoked to avoid the difficulties of perturbative QCD and by heuristic arguments [24] one chooses $\phi_5 \sim 1/5\phi_1$ with an arbitrary phase difference $\eta \sim 45°$. In principle phase differences arise also in perturbative QCD from the integration over the quark wave functions and they can be large [24]. However we should mention that there are strong objections against the dominance of pertubative QCD over non-perturbative effects to exclusive processes [25]. To evaluate non-perturbative effects one can consider diquarks, as a way to interpret higher twist effects present in many reactions. By assuming that diquark exist inside baryons as quasi elementary constituents taking part in the scattering at medium Q^2 values *only*, one is developing a consistent scheme allowing explicit computations for exclusive reactions at large angles [26]. In particular as a consequence of diquark-gluon coupling, one can break the rule of eq.(6) but the choice of the phase needed to explain the large value of A in $pp \to pp$ remains arbitrary.

Finally we briefly mention another way to produce a phase difference in perturbative QCD. It is based on the consideration of subtle Sudakhov effects which generate the so called Chromo-Coulomb Phase [27] analogous to the QED Coulomb Phase. At fixed angle one gets a factor

$$e^{-\ln^2(-s)} = e^{-\ln^2(s)} e^{i\pi \ln s} \tag{11}$$

introducing an energy dependent phase in the scattering amplitudes. There is some evidence for an oscillatory pattern [28] with energy of the pp elastic cross section at 90°as shown in Fig.14. It is also conceivable that some spin observables at fixed angle oxcillate as possibly suggested by Figs.4 and 9, but clearly more data is needed in this fascinating field of pp elastic scattering at large angles.

We now turn to a very interesting set of data on various elastic and inelastic meson-baryon cross sections at 90°and 10 GeV/c [29]. The results are reported in Fig.15 and clearly it is striking to observe that the smallest cross sections are those for the reactions which do not allow a quark interchange. For example K^+p elastic scattering has a cross section of a few nanobarns whereas K^-p has a much smaller cross section. It corresponds

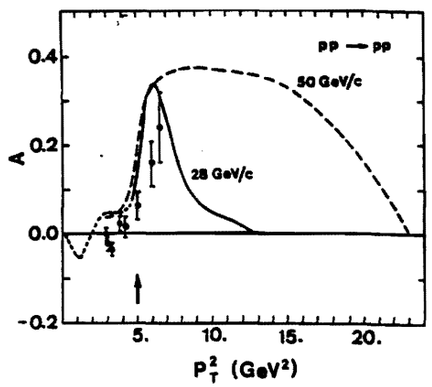

Fig.11 Model predictions for the pp analyzing power at 28 GeV/c and 50 GeV/c taken from ref. [22] (data at 28 Ge/Vc from ref.[12]).

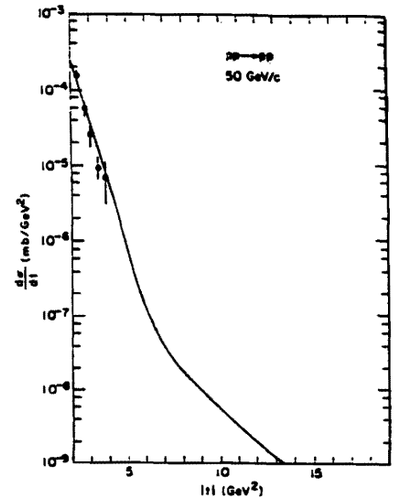

Fig.12 pp elastic data at large angles and 50 GeV/c from ref.[23] compared to the calculation from ref.[22].

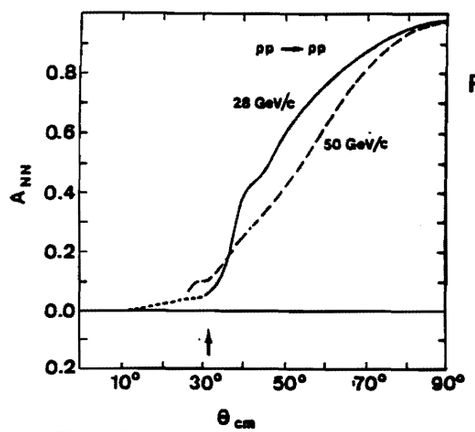

Fig.13 Model predictions for A_{NN} versus $\theta_{c.m.}$ in pp elastic scattering at 28 GeV/c and 50 GeV/c taken from ref.[22].

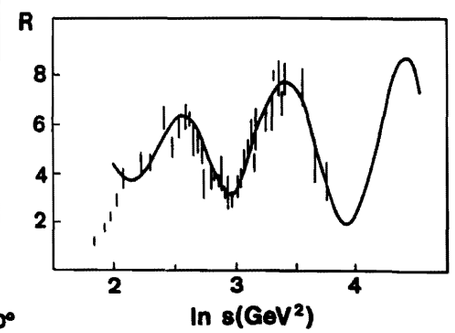

Fig.14 The quantity $R = s^{10} d\sigma/dt$ for pp elastic scattering at 90° taken from ref.[27].

to the fact that K^+ which is a $u\bar{s}$ state can interchange its u quark with one of the proton whereas K^- which is a $\bar{u}s$ state cannot. Notice also the hudge difference between pp and $\bar{p}p$, the first one allowing a maximum quark interchange and the second one none. One can also remark from Fig.15 that d quark interchange in reactions 2 and 6 leads to smaller cross sections than u quark interchange in reactions 1, 3, 5 and 7[2]. In this respect, let us recall that at 12 GeV/c np elastic scattering is about one half of pp elastic scattering [31].

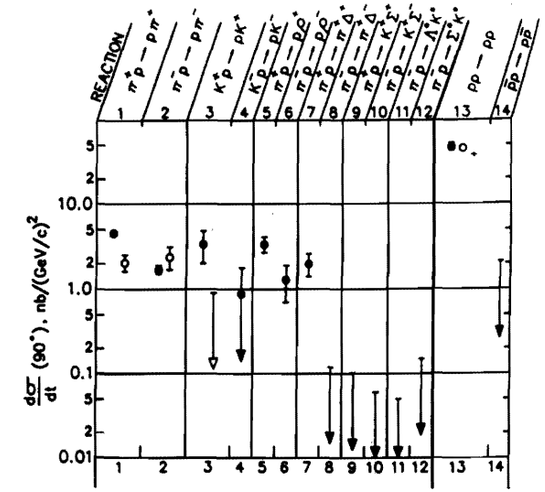

Fig.15 Values and upper limits for several two-body cross sections at 90°taken from ref.[29].

There are several other inelastic reactions where one could check the dominance of quark interchange, for example the three charge exchange reactions displayed in Fig.16.

[2] The cross section for this last reaction is smaller but it might have been under estimated. In a rather poor statistics experiment [30] it was claimed that the cross sections for $\pi^- p \to \pi^- \Delta^+$ and $\pi^- p \to \pi^- p$ have the same magnitude at 5 GeV/c but this remains to be checked.

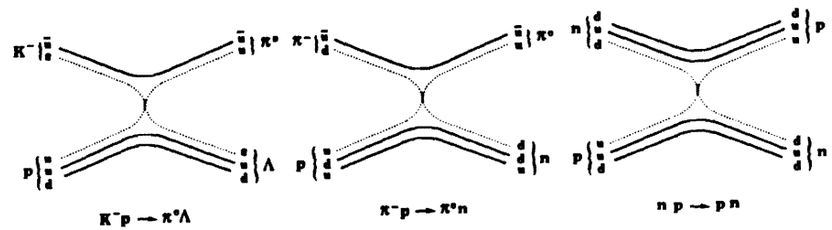

Fig.16 Three inelastic two-body reactions dominated by quark interchange indicate explicitely by the dashed lines.

From the values of the cross sections for $K^-p \to \pi^0\Lambda$ and $\pi^-p \to \pi^0 n$ known around 5 GeV/c, by using eq.(5) one can extrapolate to get their magnitudes at 10 GeV/c. We find that they turn out to be of the order of one nanobarn, that is large, but a direct confirmation from experiment is needed. Moreover, one has already observed sizeable transverse polarization effects (see Figs.5 and 17) in the large angle region for two of the reactions shown in Fig.16 and our conjecture is that these effects are deeply related to quark interchange.

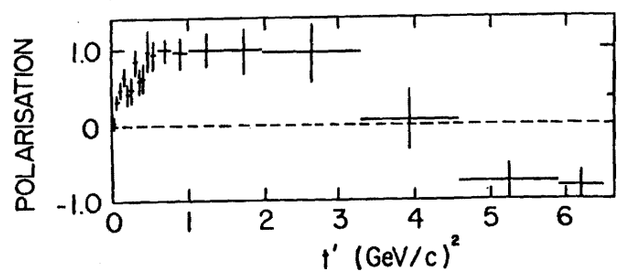

Fig.17 The Λ transverse polarization in $K^-p \to \pi^0\Lambda$ at 4.2 GeV/c reaches values of the order of + 100% at large angles (Data from ref.[32]).

3. SPIN IN INCLUSIVE REACTIONS

Let us now turn to the consideration of spin effects in inclusive reactions a rich field in itself, we will only survey. We will study different asymmetries for various reactions and we will see how they allow to test complementary dynamical features. We will start with single helicity asymmetries in lepto production and in pp collisions, whose magnitude and sign can be related, in principle, in the standard electroweak model to the coupling of the axial vector current. Then we will discuss single transverse spin asymmetries at small p_T for which a lot of data exist for hyperon production, whose theoretical interpretation is rather subtle. We will also, very briefly, consider the large p_T region and $x_F \sim 0$. Then we will give some QCD predictions for double helicity asymmetries which will be accessible to future experimental programs.

3.1. *Single helicity asymmetries*

Parity is violated in deep inelastic lepton scattering because of the $\gamma^* - Z$ interference and in the reaction $\vec{e}p \to eX$ with an unpolarized target and a longitudinally polarized electron beam, the single helicity asymmetry defined as

$$A_L = \frac{d\sigma_- - d\sigma_+}{d\sigma_- + d\sigma_+} \tag{12}$$

behaves like

$$A_L \sim \frac{G_F}{\alpha} Q^2 \tag{13}$$

where G_F is the Fermi constant and α the fine structure constant. Note that A_L is growing with Q^2 and some years ago, an heroic SLAC experiment has found at small Q^2 values [33]

$$A_L/Q^2 = (9.5 \pm 1.6)10^{-5}(GeV)^{-2} \tag{14}$$

in excellent agreement with the standard model expectation. Now in a machine like HERA, one can reach much larger Q^2 values so this asymmetry will be of the order of 20-30 % and therefore very easily accessible. Its measurement would test the presence of one (or several) intermediate neutral bosons. As an example which is taken from ref. [34] we show in Fig.18

two predictions for A_L for a fixed value of $x = Q^2/2m_p\nu$ and as a function of $y = \nu/E$ with $\nu = E - E'$ and E, E' the energy of the incoming outgoing lepton respectively. This is one of the main motivations for a high energy *ep* storage ring, but unfortunately the fact that the proton beam will be unpolarized for HERA, there will be no new information at large Q^2 about the quark helicity asymmetries Δq_i, we will consider in section 4.

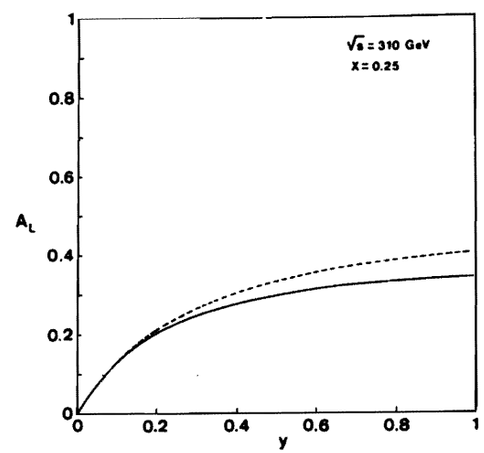

Fig.18 Predictions for A_L versus y at HERA energy. Solid curve from the standard model and dashed curve from a left-right model [35].

We will now move on to the subject of helicity dependence of proton-proton total cross section and consider the weak asymmetry defined as

$$A_L = \frac{\sigma_{tot}(+) - \sigma_{tot}(-)}{\sigma_{tot}(+) + \sigma_{tot}(-)} \tag{15}$$

where $\sigma_{tot}(\pm)$ are total $N - N$ cross sections with *one* of the nucleons in a definite helicity state $(\pm)$. This asymmetry is a direct measure of parity violation in a purely hadronic reaction. At very low energy there are several measurements, but the most accurate one was done on hydrogen at 45 MeV and yields a non-zero *negative* value [36]

$$A_L = -(1.5 \pm 0.22)10^{-7} \tag{16}$$

which provides tight constraints to theoretical estimates based on an effective parity-violating Lagrangian arising from light boson exchanges. However at Argonne, on a water target at 6 GeV/c, they found [37] a large *positive* asymmetry

$$A_L = +(26.5 \pm 6)10^{-7} \quad . \tag{17}$$

A small *positive* value $A_L = +(2.4 \pm 1.1 \pm 0.1)10^{-7}$ has also been [38] reported from a 1.5 GeV/c experiment at LAMPF. The experimental result of eq.(17) cannot be understood by assuming that the parity non-conserving $N - N$ interaction is dominated by the exchange of π, ρ and ω mesons. It leads to a value of A_L at least one order of magnitude smaller than the data, even after including the strong interaction corrections [39]. This cannot be explained either in the standard electroweak model by invoking only Z and W exchanges between the two interacting nucleons [40]. This mechanism gives also a contribution to A_L one order of magnitude smaller that the 6 GeV/c data. However it can be explained by parity violating wave function effects arising from the interaction of Z and W among the three quarks of a single nucleon [41]. This interesting idea has been successfully applied to derive a parity violating $N - N$ potential for the calculation of A_L at very low energies [42]. Finally let us mention another calculation of the interference of the strong and weak amplitudes including perturbative QCD effects [43]. These effects are too poorly know, to provide the normalization of A_L which, however, is predicted to increase strongly with energy above 2 GeV/c, in contrast with the previously mentionned parity violating wave function effect. A measurement of A_L in the energy range of the FNAL polarized beam where A_L is expected to be of the order of a few 10^{-5} would help clarifying this important question.

3.2 Single transverse spin asymmetries

Let us consider the inclusive hadronic reaction

$$a + b \rightarrow c + X \tag{18}$$

where one observes the transverse polarization state of one of the hadrons (initial of final). The simplest measurable quantity is the single transverse spin asymmetry (or up-down

asymmetry) defined as, for example if c is polarized,

$$A = \frac{d\sigma_c(\uparrow) - d\sigma_c(\downarrow)}{d\sigma_c(\uparrow) + d\sigma_c(\downarrow)} \tag{19}$$

also usually called the c polarization.

By using the generalized optical theorem one can write

$$Ad\sigma = Im(f_+^* f_-) \tag{20}$$

where $d\sigma = d\sigma_c(\uparrow) + d\sigma_c(\downarrow)$ is the corresponding unpolarized inclusive cross section described by means of f_+, the forward non-flip $3 \to 3$ helicity amplitude $ab\bar{c}_\lambda \to ab\bar{c}_\lambda$, while f_- is the forward flip amplitude $ab\bar{c}_\lambda \to ab\bar{c}_{-\lambda}$. In order to get a non-zero A, one needs *both* f_+ and f_- and moreover these two amplitudes should have a phase difference. This point is important and should be taken seriously if we want to have a real understanding of the available experimental data.

3.2.1. The fragmentation region (small p_T)

There is a large amount of significant polarization data for inclusive hyperon production as shown in Figs.19, 20 and 21. Sizeable effects and some regular behavior have been observed which may help to uncover the underlying mechanism for particle production. This was first discovered in 1976 at FNAL by studying hyperons produced by 300 GeV/c protons on a beryllium target [46] ; more specifically the Λ's produced in the fragmentation region have a large polarization perpendicular to the production plane. Over the last fifteen years a fair number of different experiments have accumulated high statistics data on inclusive lambda production which make it the best known hyperon inclusive reaction [47]. Note that all observable quantities are in general functions of three independent kinematic variables, $\sqrt{s}$ the center of mass (c.m.) energy, x_F the fraction of incident proton momentum carried by the lambda in the initial direction of the proton (in the c.m. system) and p_T the transverse momentum of the lambda relative to the initial proton direction. The beam (target) fragmentation region corresponds to $x_F \sim 0.5$ ($x_F \sim -0.5$), and in this case when one assumes that together with the lambda a kaon is also produced carrying a large positive (negative) x_F, say $x_F > 0.2$.

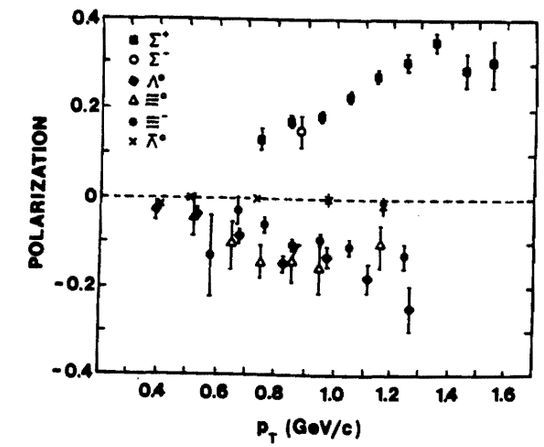

Fig.19 Transverse asymmetry (or polarization) of different hyperons produced by 400 GeV/c protons on beryllium versus p_T from ref.[44] and references therein.

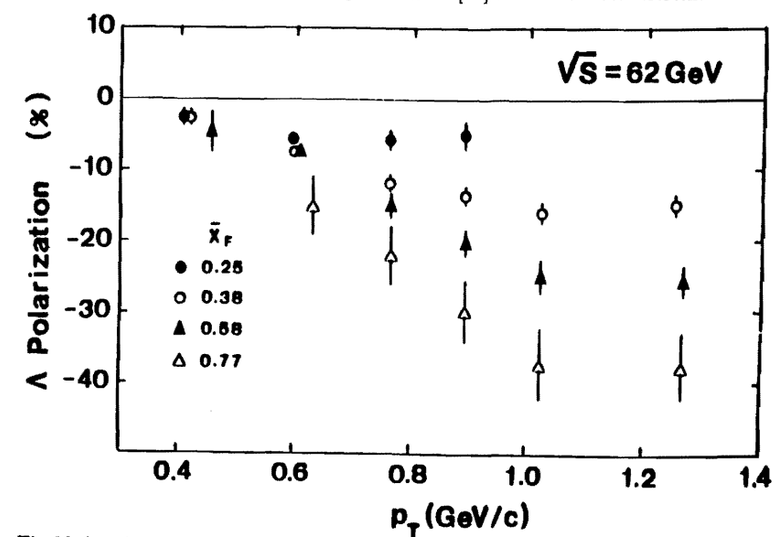

Fig.20 Λ polarization versus p_T for various x_F values at ISR energy. Data from ref.[45].

Let us now briefly recall the main features of the data in the beam fragmentation region

i) the invariant cross section $E\frac{d^3\sigma}{dp^3}$ depends, to a good approximation, only on x_F and p_T and *not* on the c.m. energy.

ii) the transverse polarization P is *negative* with respect to the direction $\vec{n} = \vec{p}_{inc} \times \vec{p}_\Lambda$.

iii) P is almost energy independent for an incident energy ranging from 12 GeV/c to 2000 GeV/c (see Fig.21).

iv) for p_T below 1 GeV/c, the magnitude of P is approximately linear with p_T with a slope increasing with x_F (see Fig.20).

v) for p_T above 1 GeV/c, the magnitude of P is independent of p_T up to $p_T \sim 3.5$ GeV/c and approximately linear on x_F.

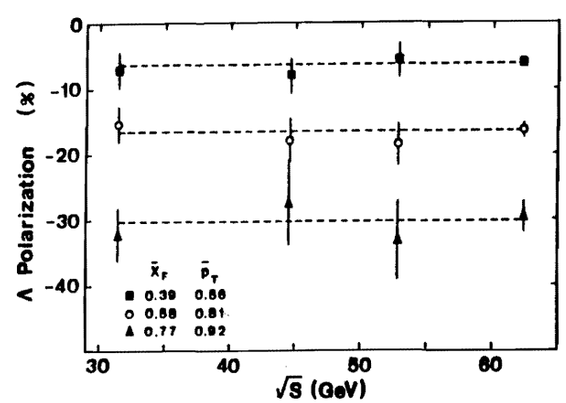

Fig.21 Λ polarization for various p_T and x_F versus $\sqrt{s}$ in the ISR energy range. Data from ref.[45].

On the theoretical side we recall that in terms of the constituent quarks, proton fragmentation into a lambda with $p_T \neq 0$ corresponds to the replacement of a valence u quark in the projectile by a strange quark s coming from the sea which must be accelerated

and must get a non zero p_T. By assuming a $SU(6)$ wave function, the (ud) system of the lambda is in a singlet state, so the polarization of the lambda is that of the strange quark.

In the Lund semi-classical fragmentation model [48], the confined linear colour field is stretched and the strange quark needed to make the final lambda with $p_T \neq 0$ is produced by an $\bar{s}s$ pair whose orbital angular momentum must be balanced by the spin of the strange quark. From this mechanism results a negative lambda polarization increasing with p_T but whose magnitude is difficult to predict.

The recombination model [49] is another approach based on classical arguments. If $\vec{F}$ is the colour force which provides the acceleration to the strange quark, this s quark of velocity $\vec{v}$ feels the effect of a Thomas precession given by $\vec{w}_T \sim \vec{F} \times \vec{v}$ which has the direction of the normal $\vec{n}$ to the hadronic scattering plane. In order to minimize the energy $\vec{s}.\vec{w}_T$ associated to this effect, the spin $\vec{s}$ of the s quark should be opposite to $\vec{w}_T$ so one expects a negative polarization in $pp \to \Lambda X$ whose magnitude is not known. In neither of these two approaches does one give a quantitative description of the invariant cross section.

We now turn to the mechanism which we believe is at work for lambda inclusive production in the fragmentation region [50]. This involves the reggeized one-pion exchange model proposed several years ago and which gives a successful description of various exclusive and inclusive reactions [51,52]. As is well known if quantum numbers allow, pion exchange generally dominates hadronic amplitudes especially at small momentum transfers. Therefore following ref.[52], we will assume that in the fragmentation region the diagram shown in Fig.22 dominates such that the multiperipheral chain reduces only to the binary reaction $\pi p \to K\Lambda$ and the total πp cross section connected by the exchange of an off-shell reggeized pion. Thus the contribution of this diagram to the cross section $pp \to \Lambda K X$ can be expressed in the following form

$$d\sigma = \frac{1}{2\sqrt{\lambda(s,m^2,m^2)}} \left[16\pi\lambda(s_1,m^2,\mu^2)\frac{d\sigma_{\pi N\to K\Lambda}}{dt_1}(s_1,t_1)\right] \cdot \left[2\sqrt{\lambda(s_2,m^2,\mu^2)}\sigma^{tot}_{\pi N}(s_2)\right] F^2(t;s_1,s_2,s)\frac{d^3p_K}{(2\pi)^3 2E_K}\frac{d^3p_\Lambda}{(2\pi)^3 2E_\Lambda} \quad (21)$$

where p_1, p_2, p_K and p_Λ are respectively the momenta of the initial protons and of the

produced kaon and lambda, m and μ being the proton and the pion masses. Moreover the *five* invariants of the reaction are defined as follows : $s = (p_1 + p_2)^2$ is the collision energy squared, $s_1 = (p_K + p_\Lambda)^2$ is the energy squared of the binary reaction, $s_2 = (p_1 + p_2 - p_K - p_\Lambda)^2$ is the invariant mass squared of X, t_1 is the invariant momentum transfer squared from the proton beam to the lambda and the mass squared of the off-shell pion is $t = (p_1 - p_K - p_\Lambda)^2$. In eq.(21), we also have the usual kinematical function $\lambda(x,y,z) = (x-y-z)^2 - 4yz$ and we denote $\frac{d\sigma_{\pi N \to K\Lambda}}{dt_1}(s_1, t_1)$ the differential cross section for the binary reaction and $\sigma^{tot}_{\pi N}(s_2)$ the πN total cross section. The function $F(t; s_1, s_2, s)$ which includes the reggeized pion propagator and describes the off mass shell behavior will be given explicitly later. The five invariants of the reaction can be reexpressed in terms of five more convenient variables, namely x_Λ and x_K the x'_Fs of the lambda and of the kaon, $p_{T\Lambda}$ and p_{TK} the corresponding transverse momenta relative to the initial proton direction (in the c.m. system) and φ the angle between the two directions $\vec{p}_{T\Lambda}$ and $\vec{p}_{TK}$.

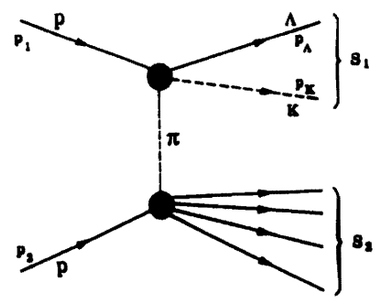

Fig. 22. Single pion exchange diagram for the process $pp \to \Lambda K X$.

It is important for our argument that in the fragmentation region, i.e. $x_\Lambda \sim 0.5$ and $x_K \sim 0.2$, the effective energy of the binary s_1 is *always much smaller* than s and, in general except for $x_K = 0$, it is reduced to values in the range of 10 GeV^2 or less. On the other hand s_2 remains of the order of s and approximately $s_2 \sim (1 - x_\Lambda - x_K)s$. Therefore from eq.(21) it results that, provided F^2 remains small when s increases, the cross section obeys *scaling* in agreement with the observed inclusive lambda spectrum. Another important kinematic observation is that t is generally not very large in the region considered, where

$p_{T\Lambda}$ and p_{TK} are small and $x_\Lambda + x_K$ not far from unity. Thus the pion will not be far off-shell. The invariant cross section for lambda production is obtained from eq.(21) after integration over the invariant phase space element of the kaon d^3p_K/E_K.

It now remains to discuss the form of $F(t; s_1, s_2, s)$. Following refs.[51,52] we will replace the pion propagator by the function

$$F(t; s_1, s_2, s) = exp\left[\left(R^2 + \alpha'_\pi ln\frac{sm^2_{TK}}{s_1 s_2}\right)(t - \mu^2)\right] \times \begin{cases} \frac{\pi\alpha'_\pi}{2}\frac{1}{\sin(\pi\alpha_\pi(t)/2)} & \text{for } |t| < |T_0| \\ \frac{\pi\alpha'_\pi}{2}\frac{\exp[R_1^2(t-T_0)]}{\sin(\pi\alpha_\pi(T_0)/2)} & \text{for } |t| > |T_0| \end{cases} \tag{22}$$

and will assume a linear parametrization $\alpha_\pi(t) = \alpha'_\pi(t - \mu^2)$ for the pion trajectory. This expression leads to the usual single and double Regge behavior in the corresponding kinematic regions and, due to the signature factor, it reduces for small t to the ordinary pion-pole propagator $1/(t - \mu^2)$. In order to avoid a too much slow decrease of F with increasing t, one imposes the following bound $R^2 + R_1^2 + \alpha'_\pi ln(sm^2_{TK}/s_1 s_2) \geq \lambda_0$. To summarize $F(t; s_1, s_2, s)$ depends on five parameters $R^2, R_1^2, \alpha'_\pi, T_0$ and λ_0 whose values were obtained in ref.[51,52] from the analysis of exclusive reactions. The calculation of the invariant cross section requires the knowledge of the binary cross section $\pi p \to K\Lambda$ at low and moderate energies for which we use an interpolation of the low energy data [53,54] for $\pi^- p \to K^0\Lambda$, for $p_{lab} < 4\ GeV/c$, in terms of an expansion of Legendre polynomials and for $p_{lab} > 4\ GeV/c$ we use a Regge parametrization of the data [55].

We must emphasize that this approach allows us to predict the ***absolute normalization*** of the invariant inclusive cross section and the comparison with experimental data of the measured Λ production by 400 GeV/c protons on hydrogen is given in ref.[50]. The theoretical predictions correspond to the set of parameters

$$R^2 = -0.55\ GeV^2\ ,\ R_1^2 = 1.25\ GeV^2\ ,\ \alpha'_\pi = 0.85\ GeV^{-2}\ ,$$
$$T_0 = -0.25\ GeV^2 \text{ and } \lambda_0 = 0.35\ GeV^{-2} \tag{23}$$

which are slightly different from those used in ref.[52] since, of course, our knowledge on the Λ inclusive spectrum has greatly improved since 1974. Note that we take $\sigma^{tot}_{\pi N}(s_2) = 24mb$,

an appropriate average value for the relevant range of s_2 under consideration. As shown in Fig.23, we get the correct absolute normalization, the right trend of the data both in x_Λ and $p_{T\Lambda}$, the best agreement occuring for $x_\Lambda \sim 0.5$. Therefore, although no doubt the fit and the model can be refined, we are confident in the validity of the fact that this model gives the dominant contribution to the cross section in the fragmentation region.

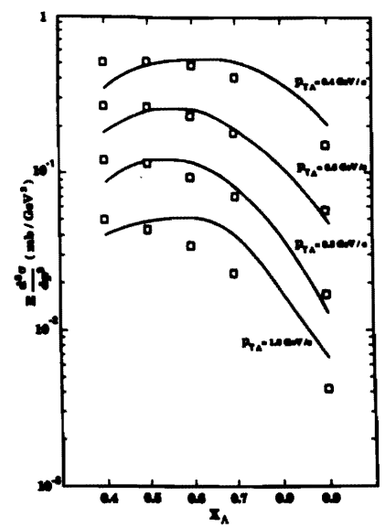

Fig.23 Inclusive lambda invariant cross section at $p_{lab} = 400$ GeV/c versus x_Λ for different $p_{T\Lambda}$ values. Solid curves are our theoretical predictions and open squares are the data representation from ref.[47] with typical errors.

A crucial test of this model is however: can it also predict the lambda transverse polarization P? Clearly it must be related to the lambda polarization P_Λ of the binary reaction $\pi p \to K\Lambda$ at low and moderate energies. There, P_Λ is known to be large and positive for $p_{lab} < 1.5\ GeV/c$ [53,54]. But at higher energies for momentum transfer $\leq -0.3\ GeV^2$ it turns large and negative [56]. Notice, now P is measured along $\vec{n} = \vec{p}_{inc} \times \vec{p}_\Lambda$ whereas in the binary reaction the lambda polarization P_Λ is observed along the normal $\vec{N} = \vec{p}_\pi \times \vec{p}_K = -\vec{p}_K \times \vec{p}_\Lambda$ to the $(K\Lambda)$ plane, in the proton (beam) rest frame. Therefore

one obtains $d\sigma P$ from eq.(21) by replacing $\frac{d\sigma}{dt_1}$ by $\cos\Phi\ P_\Lambda \frac{d\sigma}{dt_1}$ where $\cos\Phi = \frac{\vec{n}.\vec{N}}{|\vec{n}||\vec{N}|}$ i.e. the inclusive transverse polarization is obtained as a weighted average of the quantity $\cos\Phi P_\Lambda$. We parametrize the experimental polarization of $\pi^- p \to K^0\Lambda^0$ as $P = +0.5$ for $p_{lab} < 1.5\ GeV/c$, for all scattering angles expect near forward and backward directions where it should vanish. For $p_{lab} > 1.5\ GeV/c$ we use $P = 0.4\sin(-\pi t'/t'_0)$, with $t'_0 = 0.3\ GeV^2$, for $t' > -0.45\ GeV^2$ while for $t' < -0.45\ GeV^2$ we take $P = -0.4$. Here t' is the usual momentum transfer between the pion and the kaon which vanishes for forward scattering. In Fig.24 we show the results of this calculation at $p_{lab} = 400\ GeV/c$ for three x_Λ values. Since the cross section is best described for $x_\Lambda = 0.5$, we think the polarization

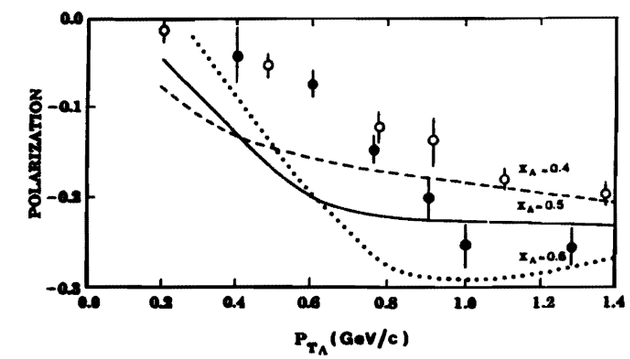

Fig.24. Comparison of the measured lambda polarization with theoretical predictions from ref.[50] at $x_\Lambda = 0.4$ (dashed curve), $x_\Lambda = 0.5$ (solid curve) and $x_\Lambda = 0.6$ (dotted curve). The open circles are FNAL data at $p_{lab} = 400\ GeV/c$ and average $x_\Lambda, \overline{x}_\Lambda = 0.44$ from ref.[47] and the solid circles are ISR data at $\sqrt{s} = 62\ GeV$ and $x_\Lambda = 0.58$ from ref.[57].

is also most reliable at the same x_Λ. For comparison we show some existing data at two different energies for nearby x_Λ values and again the agreement is remarkably good both in magnitude and sign [58]. We have also checked that the theoretical calculations for P_Λ are energy independent as it should be following iii) mentioned above. Moreover at large p_T the value of P_Λ flattens out consistently with a well established feature of the data (see v) above). The sign of P_Λ is directly related to that of P for the binary reaction for $|t'| > 0.3\ GeV^2$ and its magnitude increases with x_Λ because the cancellation from the

configurations $\cos\Phi > 0$ and $\cos\Phi < 0$ is more effective for small values of x_Λ.

In a rough way, the shape of the inclusive polarization as a function of $p_{T\Lambda}$ is the same as that of the binary as a function of t'. From this argument one can see that the mirror symmetry between the polarizations in $\pi^+p \to K^+\Sigma^+$ and $\pi^-p \to K^0\Lambda^0$ observed in ref.[56]. leads us to predict the inclusive Σ^+ polarization to be mirror symmetric to that of the Λ in accordance with observation (see Fig.19).

Also for the spectacular mirror symmetry effect observed recently at FNAL in pp collisions with polarized proton beam for π^+ and π^- inclusive production shown in Fig.25,

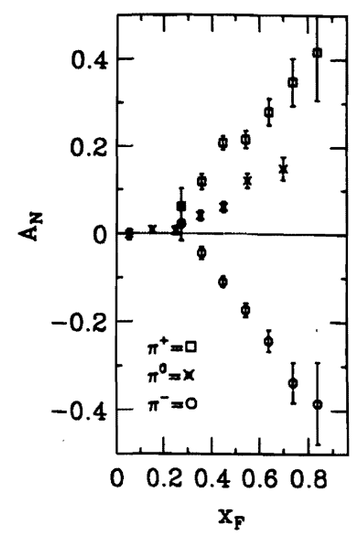

Fig.25. A_N versus x_F for π^+, π^- and π° data from ref.[59].

the model can easily account for that due to the mirror symmetry of the polarizations for $\pi^\pm p \to p\pi^\pm$ in the backward direction at low energies. Moreover we anticipate the correct sign since the binary polarization at $u \sim -0.5\ GeV^2$ is opposite to that of the inclusive at $p_T \sim 1\ GeV/c$. This opposite sign occurs because for the binary the polarization is measured along $\vec{\pi}_{in} \times \vec{\pi}_{out}$ which corresponds for the inclusive to $-\vec{p}_{inc} \times \vec{\pi}_{out}$. Finally in

$\bar{p}p$ collisions with polarized $\bar{p}$ one observes at FNAL that the polarizations for π^+ or π^- inclusive production are opposite in sign to those of π^+ or π^- in pp collisions [60]. This fact follows naturally in the model from charge conjugation at the level of the binary.

3.2.2. The central region $x_F \sim 0$ (large p_T)

The single transverse spin asymmetry at the quark level P_q is expected to be small because it should vanish in the chiral limit ($P_q \sim m_q/p_T$) and it should have a non-zero imaginary part of the quark scattering amplitude ($P_q \sim \alpha_s$). However it was shown that these simple-minded arguments do not apply if one considers non-leading twist contributions [61]. In particular A_N for $p^\uparrow p \to \gamma(\text{or } \pi)X$ at large $p_T (p_T \geq 4GeV/c)$ provides information on the twist-3 partonic distribution involving the correlation between quark fields and the gluon field strength. The absolute normalization of this new structure function is unknown and can be only determined from experimental data. For fixed p_T one expect these A_N to increase with x_F of γ or π, because higher twist contributions get enhanced at the edge of the phase space [62]. We show in Fig.26 a large effect obtained in recent data from FNAL.

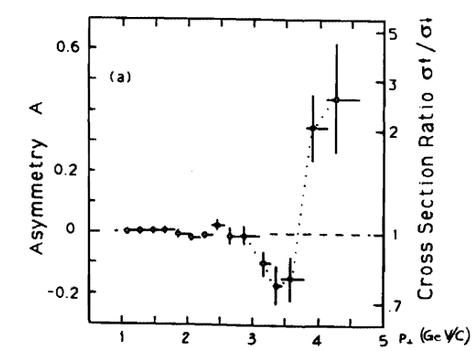

Fig.26 A versus p_T at $x_F \sim 0$ in $p^\uparrow p \to \pi^\circ X$ from ref.[60].

3.3 Double helicity asymmetries

Let us consider a single particle inclusive reaction (see eq.18) when both initial hadrons are longitudinally polarized. One can measure the double helicity asymmetry A_{LL} defined as

$$A_{LL} = \frac{d\sigma_{a(+)b(+)} - d\sigma_{a(+)b(-)}}{d\sigma_{a(+)b(+)} + d\sigma_{a(+)b(-)}} \tag{24}$$

which, in the hard scattering region, is given by

$$A_{LL} d\sigma = \sum_{ij} \frac{1}{1+\delta_{ij}} \int dx_a dx_b \left[\Delta f_i^{(a)}(x_a, Q^2)\Delta f_j^{(b)}(x_b, Q^2) + (i \leftrightarrow j)\right] \hat{a}_{LL}^{ij} d\hat{\sigma}_{ij} \tag{25}$$

where the quantities Δf's, which are the parton helicity asymmetries, will be discussed in section 4 and $\hat{a}_{LL}^{ij}$ denotes the subprocess double helicity asymmetries. The explicit expressions of these quantities for various subprocesses are given in ref.[63]. To get a rough estimate of A_{LL} one can use the following approximation

$$A_{LL} \sim \sum_{ij} \left\langle \frac{\Delta f_i}{f_i} \right\rangle \left\langle \frac{\Delta f_j}{f_j} \right\rangle \hat{a}_{LL}^{ij} \tag{26}$$

in terms of the average of the *parton polarizations* defined as $\frac{\Delta f_i}{f_i}$. It shows that, even if at the parton level $\hat{a}_{LL}^{ij}$ is as large as $\pm$ 100%, it is expected to be diluted *twice* at the hadron level since the parton polarizations are less than one in the relevant kinematic region. We will now give some examples of single inclusive reactions which will be easier to measure at high p_T because they have larger cross sections, typically at p_T=3 GeV/c direct photon production has a cross section of the order of 1 *nb*, while for jet production its value is 50 *nb*.

Direct photon production at high p_T is dominated by Compton scattering in *pp* collisions and by annihilation scattering in $\bar{p}p$ collisions. The double helicity asymmetries A_{LL} read in these approximations for *pp* collisions

$$A_{LL} = \frac{\sum_i \int [\Delta q_i(x_a)\Delta G(x_b)\hat{a}_{LL}^c d\hat{\sigma}_i^c/d\hat{t} + (x_a \leftrightarrow x_b)]}{\sum_i \int [q_i(x_a)G(x_b)\widehat{d\sigma}_i^c/d\hat{t} + (x_a \leftrightarrow x_b)]} \tag{27}$$

where $\hat{a}_{LL}^c = \frac{\hat{s}^2 - \hat{t}^2}{\hat{s}^2 + \hat{t}^2}$ and $d\hat{\sigma}_i^c/d\hat{t} = -e_i^2 \frac{\pi\alpha\alpha_s}{3\hat{s}^2}\left(\frac{\hat{s}^2+\hat{t}^2}{\hat{s}\hat{t}}\right)$ and for $\bar{p}p$ collisions

$$A_{LL} = \frac{\sum_i \int \Delta q_i(x_a)\Delta\bar{q}_i(x_b) a_{LL}^A d\hat{\sigma}_i^A/d\hat{t}}{\sum_i \int q_i(x_a)\bar{q}_i(x_b) d\hat{\sigma}_i^A/d\hat{t}} \tag{28}$$

where $\hat{a}_{LL}^A = -1$ and $d\hat{\sigma}_i^A/d\hat{t} = e_i^2 \frac{\pi\alpha\alpha_s}{\hat{s}^2}\frac{8}{9}\left(\frac{\hat{t}^2+\hat{u}^2}{\hat{t}\hat{u}}\right)$. In these expressions the integration has to be done over the appropriate parton phase space. Let us first discuss *pp* collisions.

The gluon helicity asymmetry ΔG which occurs in eq.(27) is not directly known from experiment, so we will assume it is positive and such that gluons carry about 20% of the proton spin. This can be questioned on the light of the EMC data as we will discuss below, but the measurement of A_{LL} is another way of getting some information on $\Delta G(x)$. The results are shown in Fig.27 for two different values of the c.m. production angle $\theta_{c.m.} = 45°$

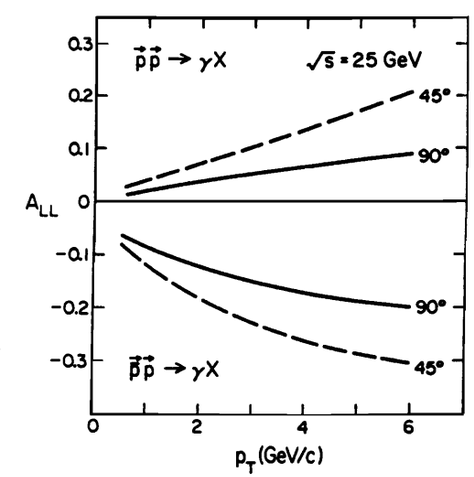

Fig.27 The double helicity asymmetry versus p_T for direct proton production at $\sqrt{s} = 25$ GeV and the different values of the c.m. production angle $\theta_{c.m.} = 45°$ and 90°.

and 90° and A_{LL} would vanish if $\Delta G = 0$ and if annihilation could be fully neglected. For $\bar{p}p$ collisions from eq.(28) we see that A_{LL} is expected to be larger because $\Delta\bar{q}$ is a valence quark asymmetry and it is negative following the sign of $\hat{a}^A_{LL}$ whose magnitude will also enhance the effect. We show the results in Fig.27 which are all increasing with p_T.

Finally, let us consider the double helicity asymmetries in pion and jet production. Cross sections for these reactions are large and many subprocesses contribute to them, i.e., $uu \to uu$, $ud \to ud$, $qg \to qg$, etc... . For most of them $\hat{a}^{ij}_{LL}$ is positive [63] so we expect A_{LL} to be positive provided Δq_i and ΔG are positive. This is in agreement with the results shown in Fig.28, except for the π^- production where the down quark asymmetry Δd, which is negative according to several models (see section 4), dominates. In all cases the magnitude of A_{LL} is growing with x_T.

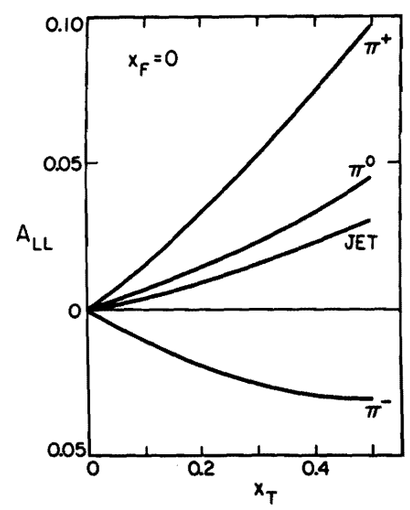

Fig.28 The double helicity asymmetry at $x_F = 0$ versus $x_T = 2p_T/\sqrt{s}$ for pion and jet production.

In conclusion we would like to stress that a large single transverse spin asymmetry has been observed at high p_T near 90° in π^0 production; it should be checked and also measured in other reactions like direct photon or jet production. We also badly need data on the A_{LL} parameter at high p_T to test the general framework behind the theoretical predictions presented here for various well defined processes. All these interesting spin tests will be hopefully well done at higher energies with the upcoming project of polarized proton beams at RHIC [63,64].

4. POLARIZED STRUCTURE FUNCTIONS

4.1. *Parton helicity asymmetries and the proton spin*

Four years ago the European Muon Collaboration (EMC) at CERN has reported the results of an accurate experiment[65] in polarized leptoproduction which has created a great deal of interest in the dynamical origin of the proton spin. The measured quantity is the double helicity asymmetry

$$A = \frac{d\sigma_{++} - d\sigma_{+-}}{d\sigma_{++} + d\sigma_{+-}} \tag{29}$$

in polarized muon-proton deep-inelastic scattering. Here $d\sigma_{++}$ and $d\sigma_{+-}$ denote the cross sections where the muon beam polarization is along the beam axis and the target polarization is either parallel (+) or antiparallel (−) to it. This measurement allows, in the scaling limit, the determination of the quantity

$$A_1(x) = \frac{\sum_i e_i^2[\Delta q_i(x) + \Delta\bar{q}_i(x)]}{\sum_i e_i^2[q_i(x) + \bar{q}_i(x)]} \tag{30}$$

where, as usual in the parton model, for a given parton, we define the *unpolarized distribution* $f = f_+ + f_-$ and the *parton helicity asymmetry* $\Delta f = f_+ - f_-$, $f_\pm$ being the distributions of this parton in a polarized nucleon with helicity either parallel (+) or antiparallel (−) to that of the parent nucleon. Clearly gluons do not contribute to the sum in eq.(30) because they don't couple to photons. We show in Fig.29 the result for A_1 on polarized protons from an earlier SLAC-Yale experiment[66] and from the recent EMC experiment over the kinematic range $0.015 \le x \le 0.7$ and $1.5 \le Q^2 \le 70 GeV^2$. The two

sets of data are fairly consistent for $x > 0.1$, but the very small x range has been uniquely explored by the EMC. Note that the expression of A_1 reads

$$A_1(x) = \frac{2xg_1(x)}{F_2(x)} \tag{31}$$

where the polarized structure function g_1 reads

$$g_1(x) = \frac{1}{2}\sum_i e_i^2[\Delta q_i(x) + \Delta\bar{q}_i(x)] \tag{32}$$

and one has a similar expression for F_2 in terms of the q_i's.

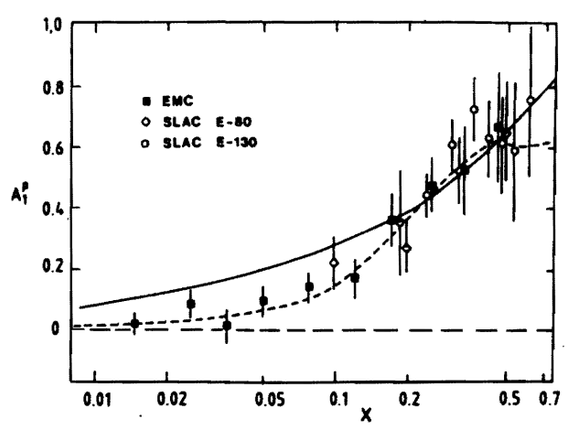

Fig.29 Data on the asymmetry A_1 versus x from ref.[65] compared with two theoretical calculations (see text).

The EMC experiment was performed on a proton target and allows to extract the proton polarized structure function $g_1^p(x)$. The EMC data are independent of Q^2 to a very high degree and yield a precise value for the integral of $g_1^p(x,Q^2)$, which is in principle a function of x and Q^2 if there are scaling violations, that is[67]

$$\int_0^1 dx\ g_1^p(x,Q^2) = 0.116 \pm 0.009\ (\text{stat.})\ \pm 0.019\ (\text{syst.})\ . \tag{33}$$

Integrals of this type are related by perturbative QCD (PQCD) through the OPE to the matrix elements of the axial vector currents of the electroweak theory. To first order in $\alpha_s(Q^2)$ one can write (we take the number of flavors $N_f = 4$)

$$\int_0^1 dx\ g_1^B(x,Q^2) = < \vec{B}\,|\,[\tfrac{1}{9}A_0 + (1-\alpha_s/\pi)\tfrac{1}{12}A_3 + (1-\alpha_s/\pi)\tfrac{1}{36}A_8]\,|\,\vec{B} > \tag{34}$$

with the singlet, triplet and octet components

$$\begin{aligned} A_0 &= \bar{u}\gamma_3\gamma_5 u + \bar{d}\gamma_3\gamma_5 d + \bar{s}\gamma_3\gamma_5 s\ , \\ A_3 &= \bar{u}\gamma_3\gamma_5 u - \bar{d}\gamma_3\gamma_5 d\ , \\ A_8 &= \bar{u}\gamma_3\gamma_5 u + \bar{d}\gamma_3\gamma_5 d - 2\bar{s}\gamma_3\gamma_5 s\ , \end{aligned} \tag{35}$$

where $|\vec{B}>$ is any longitudinally polarized baryon of the $1/2^+$ octet. By making use of $SU(3)$ (which is good to the level of at least 10%) and the experimental knowledge of baryon semi-leptonic decays, we can apply (34) to the proton and we get

$$\begin{aligned} \int_0^1 dx\ g_1^p(x,Q^2) &= \tfrac{1}{18}\left[(9F-D) - \frac{\alpha_s(Q^2)}{\pi}(3F+D)\right] + \tfrac{1}{3} < \vec{p}|\bar{s}\gamma_3\gamma_5 s|\vec{p} > \\ &= (0.186 \pm 0.005) + \tfrac{1}{3} < \vec{p}|\bar{s}\gamma_3\gamma_5 s|\vec{p} > \end{aligned} \tag{36}$$

where we have taken[68] $F = 0.477 \pm 0.011$, $D = 0.755 \pm 0.011$ and $\alpha_s(Q^2) = 0.27$. The Ellis-Jaffe sum rule[69] can be obtained from eq.(36) by assuming, following the quark model (QM) prediction, $< \vec{p}|\bar{s}\gamma_3\gamma_5 s|\vec{p} >= 0$. One immediately realizes that the experimental determination (33) is inconsistent with this prediction by 3.5 standard deviations. By comparing eq.(33) with eq.(36) one deduces that

$$< \vec{p}|\bar{s}\gamma_3\gamma_5 s|\vec{p} >= -0.220 \pm 0.065 \tag{37}$$

namely, strange quarks inside a proton carry a large fraction of the proton spin. As a consequence, one also finds that the matrix element of A_0 which measures the total amount of the proton spin carried by quarks and antiquarks reduces to -0.02 ± 0.24 compared to unity, a value expected in the naive QM. Therefore it is very surprizing to conclude that the *proton spin is not carried by the quarks*. Before going to the arguments based on

experimental facts one can oppose to eq.(37), let us recall its interpretation in terms of the anomaly of the axial vector current. According to this observation first made in ref.[70] and reexamined later in refs.[71] and [72], the Δq_i 's, defined as first moments of the $\Delta q_i(x)'s$, occuring in the naive parton model, are replaced by

$$\Delta q_i' = \Delta q_i - \frac{\alpha_s}{2\pi}\Delta G \tag{38}$$

where ΔG is also defined as the integral over x of $\Delta G(x)$. This correction results from the box graph in virtual photon-virtual gluon elastic scattering. This suggestion has been criticized on various aspects and for a general discussion about the quark and the gluon content of the proton spin and also recent references on this subject, see ref.[73]. Anyway, if one assumes that eq.(38) holds one can hope to restore the agreement between eq.(33) and eq.(36) where Δs is replaced by $\Delta s'$ provided $\Delta s = 0$ and $\Delta G \sim (0.22)2\pi/\alpha_s$ which is a large number. As a consequence, one should expect a new phenomenology of spin effects at short distances driven by this sizable positive gluon polarization i.e. $\Delta G \sim 6-7$, and if genuine, this effect should be seen directly in future hadronic collisions spin experiments. For hadronic reactions, in particular for pp collisions, the existing polarized proton (antiproton) beam at FNAL has already yielded very interesting results[60] for various inclusive reactions and hopefully it is expected to operate for some more years[74]. There is also a new very exciting project for polarized protons at RHIC[63,64] which would allow, given the high anticipated luminosity ($\mathcal{L} = 2.10^{32} cm^{-2} sec^{-1}$) and the large beam polarization ($P = 70\%$) to test various physics issues. For example, it will be possible to determine directly the magnitude and the sign of the gluon polarization from the measurement of the double helicity asymmetry A_{LL} (see eq.(27) with both proton beams longitudinally polarized in jet or direct photon production at large p_T. For illustration we show in Fig.30 different predictions for A_{LL} in $pp \to \gamma X$ together with the expected experimental accuracy.

Now let us return to the crucial question : is eq.(37) really believable? There is a strong argument[77] againt a large *measured* Δs (i.e. $\Delta s'$ in eq.(38)) from the experimental data on charm production in neutrino DIS [76,77] which provides a direct knowledge on the

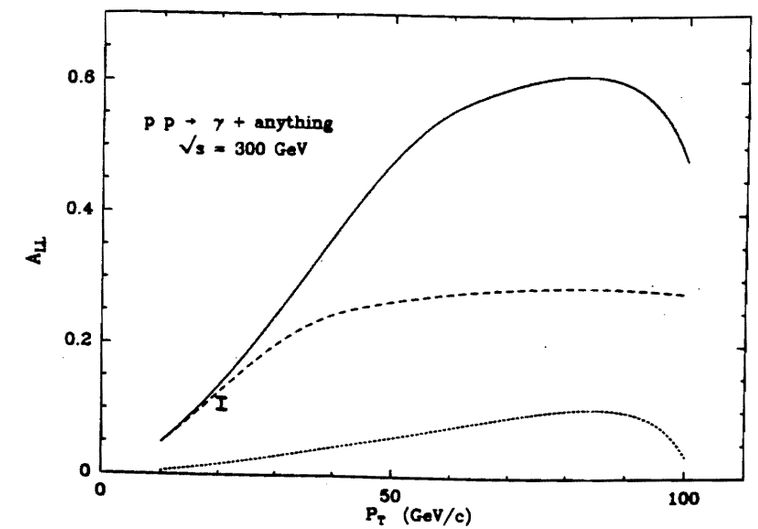

Fig.30 Predicted A_{LL} with a large ΔG for $\sqrt{s} = 300GeV$ as a function of p_T, for two different values of the c.m. production angle:$\theta_{c.m.} = 90°$ (dashed curve),$\theta_{c.m.} = 45°$ (solid curve). The small-dashed curve corresponds to a standard ΔG and $\theta_{c.m.} = 90°$. The error bar indicates RHIC sensitivity at $p_T = 20GeV/c$ and for $\Delta y = 1, \Delta\phi = 2\pi, \Delta p_T = 1GeV/c$ bin (taken from ref.[64]).

strange quark content of the proton. There are serious indications, both experimental and theoretical in favor of the following Regge behavior of the sea distributions

$$\bar{q}_\pm(x, Q^2) = (1-x)^p \sum_k C_\pm^{(k)}(Q^2) x^{-\alpha_k(0)} \tag{39}$$

where $\alpha_k(0)$ is the intercept of the k Regge pole. The leading term is the Pomeron for which $\alpha_P(0) = 1$ and the Regge residues are positive and such that $C_+^{(P)} = C_-^{(P)}$, i.e. the Pomeron coupling is spin independent. In eq.(39) p is a large number related to the high x behavior. The data of refs.[76,77] can be very well parametrized as

$$x\bar{q}(x) = (A + Bx)(1-x)^p \tag{40}$$

and one finds

$$A = 0.135 \pm 0.006 \ , \quad B = 0.53 \pm 0.22 \ , \quad p = 8.25 \pm 0.76 \ . \tag{41}$$

Therefore as a consequence of ***positivity*** one easily derives the following restrictive bound

$$|\Delta s| \leq \frac{B}{p+1} = 0.057^{+0.023}_{-0.057} \tag{42}$$

which implies using eq.(36)

$$\int_0^1 dx \ g_1^p(x, Q^2) \geq 0.172^{+0.018}_{-0.009} \tag{43}$$

in strong disagreement with eq.(33). One can check that this conclusion remains even using parametrizations more complicated than eq.(40) and all counter-examples proposed so far[78] are totally unrealistic[79] as we will see in the following illustration.

It has been claimed recently[80] that one can have at the same time a strangeness content of the proton such that the momentum fraction carried by the strange quarks, i.e. $\int xs(x)dx$, small say $\sim 3\%$ in accordance with experiment, while their spin fraction Δs could be as much as 20%. To avoid the positivity bound mentioned above, the authors of ref.[80] propose to use the following parametrization

$$xs(x) = A(1-x)^p + C(1-bx)(1-x)^{p'} \tag{44}$$

where the second term, which has a non-perturbative origin, is such that $b = p' + 2$, so it does not contribute to the momentum sum rule, and $p << p'$. They actually take $p = 5$ and $p' = 12$ and we see on Fig.31, that this choice leads to a very poor fit (fit 1) of the most recent CCFR data[82] whereas a better fit (fit 2) is obtained for $C = 0$ and $p = 11.1 \pm 0.7$ which obviously leads to $B = 0$ in eq.(40) and consequently $|\Delta s| = 0$!

There is another very important sum rule called the Bjorken sum rule[83] which can be directly obtained from eq.(34) and reads

$$\int_0^1 [g_1^p(x) - g_1^n(x)]\, dx = (0.205)\left[1 - \alpha_s/\pi + a(\alpha_s/\pi)^2 + b(\alpha_s/\pi)^3\right] \tag{45}$$

where the next-next to leading order corrections (three loops corrections) were calculated in ref.[84] and turn out to be rather small, since for $N_f = 3$ one has $a = -3.58$ and $b = -20.21$. This sum rule is independent of Δs but it was never tested since $g_1^n(x)$, the neutron polarized structure function, has not been measured yet. If the EMC result is correct, the validity of this sum rule leads one to predict for $g_1^n(x)$ large and negative values in the low-x region.

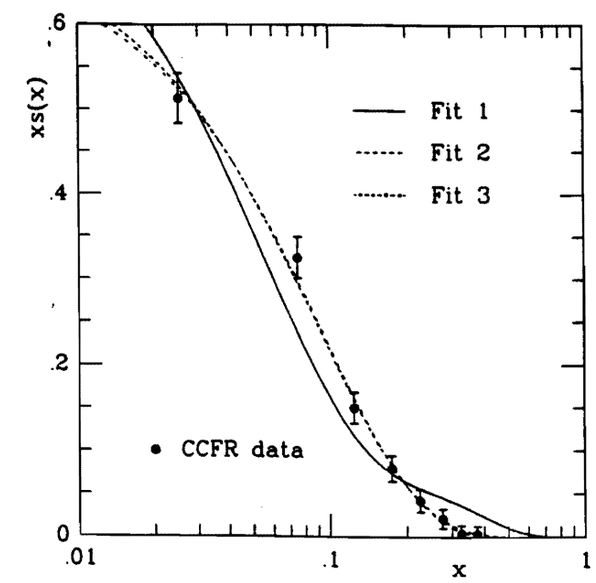

Fig.31 The curves for $xs(x)$ resulting from the fits discussed in the text compared to the CCFR data (taken from ref.[81]).

Although tests of sum rules are important, even more restrictive is the comparison of the distribution itself with experimental observation. In Fig.29 the solid curve is a quark-parton model calculation[85] which satisfies the Bjorken sum rule and thus perturbative QCD, while the dashed curve is the prediction of the MQM/QGD approach[86] and gives

a fair description of the data both at small and large x. In this approach the neutron asymmetry A_1^n is predicted to be very small and positive so the Bjorken sum rule is anticipated to be badly violated. From the NMC discovery $\overline{d} >> \overline{u}$, it was proposed[87] that this simple fact can also imply a flavor asymmetry for the light-quark sea helicity distributions i.e. $\Delta\overline{u} \neq \Delta\overline{d}$. In this approach, the quantitative effect given by $\overline{d}(x) - \overline{u}(x) = (1-x)^7$ accounts for the Ellis-Jaffe sum rule defect discussed above and predicts a large violation of the Bjorken sum rule. This burning question is a strong enough motivation to justify several new projects at CERN[88], HERA[89] and SLAC[90] to measure *both* g_1^p and g_1^n.

Finally we will consider the *transverse* spin dependent structure function, the so-called g_2, which can be measured in leptoproduction with a longitudinally polarized lepton beam on a transversely polarized nucleon target. There are no data for such an experimental situation but if there were, it would allow one to extract the quantity $g_1(x) + g_2(x)$. The literature contains several groundless conjectures like, $g_2(x) \equiv 0$ or $g_1(x) + g_2(x) \equiv 0$, etc... but recently our theoretical knowledge on $g_2(x)$ has been reviewed and clarified[45]. Whereas $g_1(x)$ is leading twist (i.e. twist-2) only, $g_2(x)$ is more complicated. First, it has a twist-2 contribution $g_2^{ww}(x)$ which is simply related to $g_1(x)$ by the Wandzura-Wilezek sum rule[92]

$$g_1(x) + g_2^{ww}(x) = \int_x^1 \frac{dy}{y} g_1(y) \tag{46}$$

and satisfies automatically the Burkhardt-Cottingham sum rule[95]

$$\int_0^1 g_2^{ww}(x)dx = 0 \ . \tag{47}$$

Second, it has a twist-3 contribution $\overline{g}_2(x)$ which is related to spin-dependent quark-gluon interacting and need not to be negligible. Actually in the bag model it turns out to be large and of opposite sign to $g_2^{ww}(x)$ (see Fig.32). Clearly experimental data on this quantity are badly needed and we hope it will be also obtained in the forthcoming polarized deep inelastic scattering experiments[88,89,90].

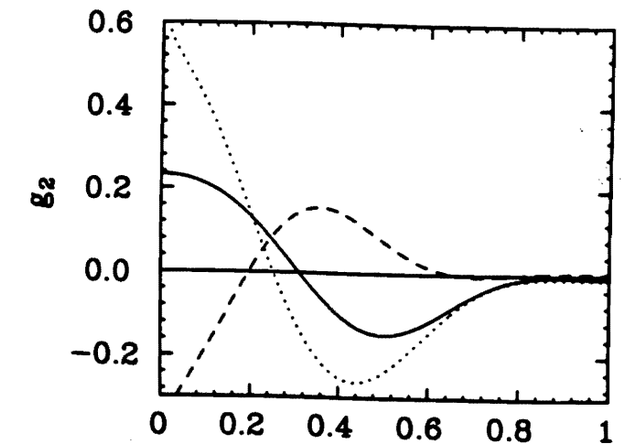

Fig.32 Predicted proton transverse structure function $g_2(x)$ in the bag model. The dotted line is the twist-2 contribution g_2^{ww}, the dashed line is twist-3 $\overline{g}_2$ and the solid line is the sum of the two (taken from ref.[91]).

4.2. *The transversity distribution and the Drell-Yan process*

Recent progress has been made in understanding transverse spin effects as already mentioned briefly in the previous section when we discussed the structure function g_2. One can make one more step in trying to answer the specific question: what is the transversity distribution of quarks inside a transversely polarized proton? The answer[96,97] is obtained by looking at the chiral structure of the parton model for the description of deep inelastic scattering and Drell-Yan production of lepton pairs. The corresponding diagrams are shown in Fig.33 and Fig.34 where it is clear that the chirality of the quark participating in the hard scattering process is conserved. In the case of deep inelastic scattering this has the *further* consequence that the *quark lines entering and leaving the nucleon are of a single chirality*. Only two independent quark-nucleon amplitudes enter the description of

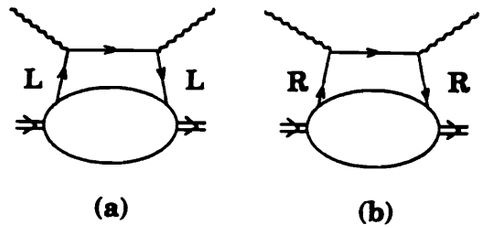

Fig.33 Chiral structure of deep inelastic scattering.

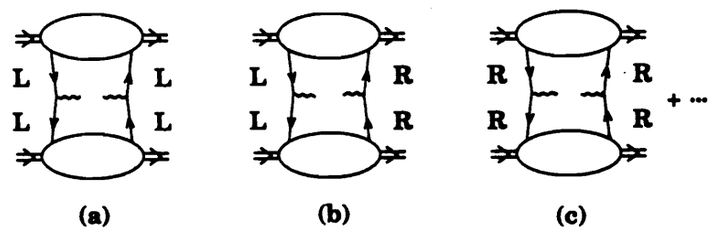

Fig.34 Chiral structure of Drell-Yan production of lepton pairs.

Fig.35 Left- and right-handed chiral even quark distributions whose sum and difference give $f_1(x,Q^2)$ and $g_1(x,Q^2)$ respectively.

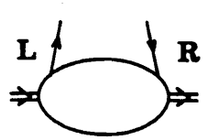

Fig.36 Chiral odd quark distribution which gives $h_1(x,Q^2)$.

deep inelastic scattering, for each flavor of quark and antiquark, one involving left-handed quarks, the other right-handed, as shown in Fig.35. They are the two chiral even quark contributions. The average over chirality gives the quark momentum distribution, $f_1(x,Q^2)$, simply related to F_2. The difference gives the chirality (or helicity) weighted quark momentum distribution $g_1(x,Q^2)$, discussed in section 4.1. and which is the dominant contribution to the spin asymmetry from a longitudinally polarized target.

Now let us turn to Drell-Yan. As always, the quark chirality is conserved in the hard part of the diagram. However, it is clear from Fig.34 that the *chirality of the quark lines entering and leaving a given nucleon need not be the same.* This allows us to define a new quark distribution, shown in Fig.36. Since the quark chirality flips and since chirality $\equiv$ helicity, up to mass terms or further hard interactions, this new distribution will be important when the nucleon helicity flips, i.e. in a transverse asymmetry. Thus there is a new structure function, $h_1(x,Q^2)$, for each flavor of quark and antiquark, which measures the quark momentum distribution in a transversely polarized nucleon weighted by ± 1 depending on whether the quark is polarized parallel or antiparallel to the nucleon. $h_1(x,Q^2)$ cannot be measured in deep inelastic scattering (except as the coefficient of a small quark mass correction) but it appears in the transverse asymmetry for Drell-Yan processes at the dominant-scaling-order. h_1 is chiral odd because it measures the correlation between left and right-handed quarks. It is leading twist like f_1 and g_1 and is, as well as, a fundamental structure function. It gives the transversity distribution of quarks and there is no reason to expect it to be small. On the contrary, in the bag model the calculation indicates that it is larger than g_1 as shown in Fig.37.

Finally let us comment on how to determine $h_1(x)$. As pointed out in refs.[94,95], $h_1(x)$ can be best measured in Drell-Yan production of lepton pairs with both proton beams transversely polarized. As an illustration we show in Fig.38 A_{TT}/a_{TT}, the ratio of the double transverse asymmetry A_{TT} to the parton asymmetry a_{TT}, which depends critically on h_1, for quarks and antiquarks. This exciting measurement will be also accessible with the polarized pp collider at RHIC[63,64].

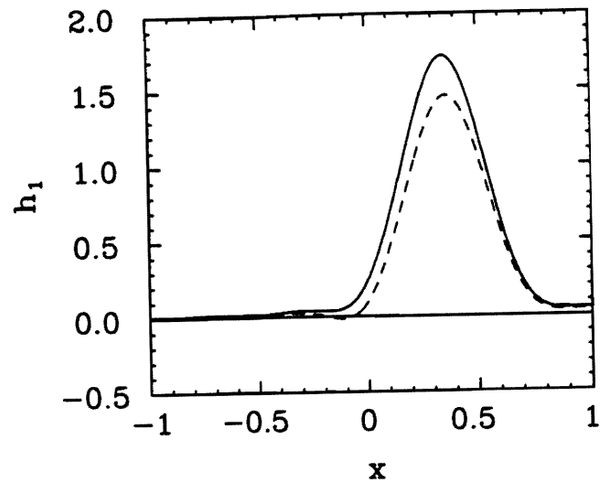

Fig.37 $h_1(x)$ versus x in the bag model (solid curve). The dashed curve represents $g_1(x)$ (taken from ref.[95]).

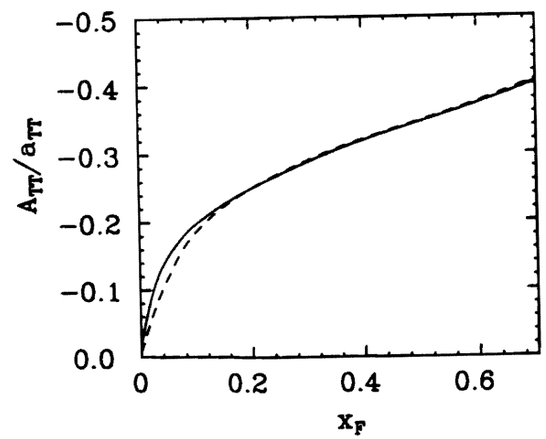

Fig.38 A_{TT}/a_{TT} for $p^{\uparrow}p^{\uparrow} \to \mu^+\mu^- X$ at $\sqrt{s} = 100GeV$ versus x_F for two values of the lepton pair mass $M = 7GeV$ (solid curve), $M = 5GeV$ (dashed curve) (taken from ref.[96]).

5. CONCLUDING REMARKS

The observation of large polarization effects in different areas of medium and high energy particle physics shows that spin degrees of freedom play a significant role in hadron dynamics. Recent data on polarized deep inelastic scattering have generated new insights in the fundamental problem of the spin structure of the proton which remain to be clarified by future data. Polarization is also a useful tool to study electroweak interactions by means of parity violation effects which could uncover new physics beyond the standard model. In pure hadronic collisions as we have seen sizeable spin effects occur for inclusive reactions both in fragmentation and central regions and for exclusive reactions mainly at large scattering angles. For short distance physics the spin properties of hadron constituents are crucial and spin effects should discriminate between challenging models. Finally we believe that polarization phenomena is now hitting very exciting frontier research areas in high energy physics.

ACKNOWLEDGMENTS

I would like to thank the organizers of this RCNP-Kikuchi School, and in particular its chairman Prof. M. Fujiwara, for their kind hospitality.

REFERENCES

[1] For an overview, see C. BOURRELY, E. LEADER and J. SOFFER, *Phys. Rep.* **59** (1980) 95.

[2] A. WICKLUND et al., Contribution to Proc. 17 th. Int. Conference on High Energy Physics, London, 1974 ed. J. SMITH.

[3] M.SVEC, A. DE LESQUEN and L. VAN ROSSUM, *Phys. Lett.* **B220** (1989) 653.

[4] G. FIDECARO et al., *Nucl. Phys.* **B173** (1980) 513.

J. SNYDER et al., *Phys. Rev. Lett.* **41** (1978) 781 ; *Phys. Rev.* **D22** (1980) 553.

[5] C. BOURRELY, J. SOFFER and T.T. WU, *Phys. Rev.* **D19** (1979) 3249 and *Nucl. Phys.* **B247** (1984) 15.

C. BOURRELY, H.A. NEAL, H.A. OGREN, J. SOFFER and T.T. WU, *Phys. Rev.* **D26** (1982) 1781.

[6] J.V. ALLABY et al., *Nucl. Phys.* **B52** (1973) 316.

[7] F.Z. KHIARI et al., *Phys. Rev.* **D39** (1989) 45.

[8] Y. MAKDISI et al., *Phys. Rev. Lett.* **45** (1980) 1529.

[9] D.G. CRABB et al., *Phys. Rev. Lett.* **65** (1990) 3241.

[10] LANDOLT-BORNSTEIN vol. 7 (1973) edited by H. SCHOPPER (Springer-Verlag, Berlin).

[11] A.C. FERNOW and A.D. KRISCH, *Ann. Rev. Nucl. Sci.* **31** (1981) 107.

[12] P.R. CAMERON et al., *Phys. Rev.* **D32** (1985) 3070.

[13] G. COURT et al., *Phys. Rev. Lett.* **57** (1986) 507 and references therein.

[14] G. FARRAR, *Phys. Rev. Lett.* **53** (1984) 28.

[15] H. AIHARA et al., *Phys. Rev. Lett.* **57** (1986) 404.

[16] C. BAGLIN et al., *Phys. Lett.* **B225** (1989) 296.

[17] B.R. BALLER et al., *Phys. Rev. Lett.* **60** (1988) 1118.

[18] S.J. BRODSKY and G.P. LEPAGE, *Phys. Rev.* **D24** (1981) 2848.

[19] I.P. AUER et al., *Phys. Rev.* **D34** (1986) 1.

[20] G. FARRAR, S. GOTTLIEB, D. SIVERS and G. THOMAS, *Phys. Rev.* **D20** (1979) 202.

S.J. BRODSKY, C. CARLSON and H.J. LIPKIN, *Phys. Rev.* **D20** (1979) 2278.

[21] G. NARDULLI, G. PREPARATA and J. SOFFER, *Nuovo Cimento* **A83** (1984) 361.

[22] C. BOURRELY and J. SOFFER, *Phys. Rev. Lett.* **54** (1985) 760 ;

C. BOURRELY and J. SOFFER, *Phys. Rev. Lett.* **D35** (1987) 145.

[23] Z ASA'D et al., *Nucl. Phys.* **B255** (1985) 273.

[24] G. FARRAR, *Phys. Rev. Lett.* **56** (1986) 1643 ;

E. MAINA and G. FARRAR, *Phys. Lett.* **206B** (1988) 120.

[25] N. ISGUR and Ch. LLEWELLYN SMITH, *Nucl. Phys.* **B317** (1989) 526.

[26] M. ANSELMINO, P. KROLL and B. PIRE, *Z. Phys.* **C36** (1988) 89.

[27] B. PIRE and J. RALSTON, *Phys. Lett.* **B117** (1982) 233.

[28] A.W. HENDRY, *Phys. Rev.* **D23** (1981) 2075.

[29] B.R. BALLER et al., *Phys. Rev. Lett.* **60** (1988) 1118.

[30] P.J. CARLSON et al., *Nuovo Cimento* **A62** (1981) 196.

[31] J.L. STONE et al., *Phys. Rev. Lett.* **38** (1977) 1315.

[32] F. MARZANO et al., *Nucl. Phys.* **B123** (1977) 203.

[33] Y. PRESCOTT et al., *Phys. Lett.* **B84** (1979) 524.

[34] P. CHIAPPETTA, J. Ph. GUILLET and J. SOFFER, *Nucl. Phys.* **B262** (1985) 187.

[35] V. BARGER, E. MA and K. WHISNANT, *Phys. Rev.* **D28** (1983) 1618 and references therein.

[36] S. KISTRYN et al., *Phys. Rev. Lett.* **58** (1987) 1616.

[37] N. LOCKYER et al., *Phys. Rev. Lett.* **45** (1980) 1821.

[38] V. YUAN et al., *Phys. Rev. Lett.* **57** (1986) 1680.

[39] A. BARROSO, Proc. of the 8 th. Int. Workshop on weak interactions and neutrinos, Javea, Spain 6-11 sept. 1982 (World Scientific) p. 571.

[40] P. CHIAPPETTA, J. SOFFER and T.T. WU, J. Phys. G : *Nucl. Phys.* **8** (1982) L93.

[41] G. NARDULLI and G. PREPARATA, *Phys. Lett.* **B117** (1982) 445 ; ibid **B137** (1984) 111.

[42] G. NARDULLI, G. PREPARATA, E. SCRIMIERI and J. SOFFER, *Phys. Lett.* **B122** (1983) 329.

[43] T. GOLDMAN and D. PRESTON, *Phys. Lett.* **B168** (1986) 415.

[44] C. WILKINSON et al., *Phys. Rev. Lett.* **58** (1987) 855.

[45] A.M. SMITH et al., *Phys. Lett.* **B185** (1987) 209.

[46] G. BUNCE et al., *Phys. Rev. Lett.* **36** (1976) 1113.

[47] L.G. PONDROM, *Physics Reports* **122** (1985) 57;

B. LUNDBERG et al., *Phys. Rev.* **D40** (1989) 3557.

[48] B. ANDERSSON, G. GUSTAFSON, G. INGELMAN and T. SJOSTRAND, *Physics Reports* **97** (1983) 31 and references therein.

[49] T. DE GRAND, J. MARKKANEN and H. MIETTINEN, *Phys. Rev.* **D32** (1986) 2445 and references therein.

[50] J. SOFFER and N. TORNQVIST, *Phys. Rev. Lett.* **68** (1992) 907.

[51] K.G. BORESKOV, A.B. KAIDALOV and L.A. PONOMAREV, Soviet, *J. Nucl. Phys.* **19** (1974) 565 ;

L.A. PONOMAREV, *Soviet, J. Part. Nucl.* **7** (1976) 70 and references therein.

[52] A.V. TURBINER, Soviet, J. Nucl. Phys. **22** (1976) 551.

[53] R.D. BAKER et al., *Nucl. Phys.* **B141** (1978) 29.

[54] D.H. SAXON et al., *Nucl. Phys.* **B162** (1980) 522.

[55] H. NAVELET and P.R. STEVENS, *Nucl. Phys.* **B104** (1976) 171.

[56] C.E. WARD et al., *Phys. Lett.* **B48** (1974) 471;

A. SNYDER et al., *Phys. Rev.* **D21** (1980) 599.

[57] A.M. SMITH et al., *Phys. Lett.* **B185** (1987) 209.

[58] The effect of the Σ^0 contamination arising from the decay $\Sigma^0 \to \Lambda^0 + \gamma$, suggests that one underestimates by $10 - 20\%$ the magnitude of P for directly produced Λ^0 (see M. SULLIVAN et al., *Phys. Lett.* **B142** (1984) 451).

[59] D.L. ADAMS et al., *Phys. Lett.* **B264** (1991) 462.

[60] A. YOKOSAWA, Proceedings of the XXI International Symposium on Multiparticle Dynamics, Wuhan, The People's Republic of China, Sept. 23-27, 1991, World Scientific (Editors Wu Yuanfang and Liu Lianshou) p. 545.

[61] A.V. EFREMOV and O.V. TERYAEV, *Phys. Lett.* **B150** (1985) 383, and references therein.

[62] J. QIU and G. STERMAN, *Phys. Rev. Lett.* **67** (1991) 2264.

[63] C. BOURRELY, J.Ph. GUILLET and J. SOFFER, *Nucl. Phys.* **B361** (1991) 72.

[64] G. BUNCE et al., *Particle World* **3** (1992) 1.

[65] J. ASHMAN et al., *Phys.Lett.* **B206** (1988) 364 ; *Nucl.Phys.* **B328** (1989) 1.

[66] G. BAUM et al., *Phys. Rev. Lett.* **51** (1983) 1135.

[67] V. HUGHES et al., *Phys. Lett.* **B212** (1988) 511.

[68] M. BOURQUIN et al., *Z. Phys.* **C21** (1983) 27.

[69] J. ELLIS and R.L. JAFFE, *Phys. Rev.* **D9** (1974) 1444.

[70] A.V. EFREMOV and O.V. TERYAEV, Preprint JINR EL-88-287 (unpublished).

[71] G. ALTARELLI and G.G. ROSS, *Phys. Lett.* **B212** (1988) 391.

[72] R. CARLITZ, J.C. COLLINS and A.H. MUELLER, *Phys. Lett.* **B214** (1988) 229.

[73] A.V. EFREMOV, J. SOFFER and N. TÖRNQVIST, *Phys. Rev.* **D44** (1991) 1369.

[74] N. AKCHURIN et al., Proton Spin Structures Studies in Hyperon Inclusive Production, FNAL proposal, March 1992.

[75] G. PREPARATA and J. SOFFER, *Phys. Rev. Lett.* **61** (1988) 1167 (see also *Phys. Rev. Lett.* **62** (1989) 1213).

[76] H. ABRAMOWICZ et al., *Z. Phys.* **C25** (1984) 29.

[77] D. ALLASIA et al., *Z. Phys.* **C28** (1985) 321.

[78] J. ELLIS and M. KARLINER, *Phys. Lett.* **B213** (1988) 73.

[79] G. PREPARATA, Ph. RATCLIFFE and J. SOFFER, *Phys. Lett.* **B231** (1989) 483 ; *Phys. Rev.* **D42** (1990) 930.

[80] B.L. IOFFE and M. KARLINER, *Phys. Lett.* **B247** (1990) 387.

[81] G. PREPARATA, Ph. RATCLIFFE and J. SOFFER, *Phys. Lett.* **B273** (1991) 306.

[82] C. FOUDAS et al. CCFR Collaboration, *Phys. Rev. Lett.* **64** (1990) 1207.

[83] J.D. BJORKEN, *Phys. Rev.* **148** (1966) 1467.

[84] S.A. LARIN and J.A.M. VERMASEREN, *Phys. Lett.* **B259** (1991) 345.

[85] R. CARLITZ and J. KAUR, *Phys. Rev. Lett.* **38** (1977) 673.

[86] A. GIANNELLI, L. NITTI, G. PREPARATA and P. SFORZA, *Phys. Lett.* **B150** (1985) 214.

[87] F. BUCCELLA and J. SOFFER, *Preprint CPT-92/P.2706.*

[88] The Spin Muon Collaboration (SMC) CERN/SPSC 88-47, SPSC/P242, 22 december 1988.

[89] P. MILNER, AIP Conference Proceedings n° 223, Polarized Collider Workshop, (Editors J. Collins, S. Heppelmann and R.W. Robinett), p. 305.

[90] P. SOUDER, AIP Conference Proceedings n° 223, Polarized Collider Workshop, (Editors J. Collins, S. Heppelmann and R.W. Robinett), p. 315.

[91] R.L. JAFFE, *Comments Nucl. Part. Phys.* **19** (1990) 239.

R.L. JAFFE and X. JI, *Phys. Rev.* **D43** (1991) 724.

[92] W. WANDZURA and F. WILCZEK, *Phys. Lett.* **B172** (1977) 195.

[93] H. BURKHARDT and W.N. COTTINGHAM, *Ann. Phys. (N.Y.)* **56** (1970) 453.

[94] J.P. RALSTON and D.E. SOPER, *Nucl. Phys.* **B152** (1979) 109.

J.L. CORTES, B. PIRE and J.P. RALSTON, *Z. Phys.* **55** (1992) 409.

[95] R.L. JAFFE and X. JI, *Phys. Rev. Lett.* **64** (1991) 724.

R.L. JAFFE and X. JI, *Nucl. Phys.* **B375** (1992) 527.

[96] X. JI, *Phys. Lett.* **B234** (1992) 137.